Techno-economic assessment of an automated lithium-ion battery module disassembly process

Investigating the optimal level of automated disassembly

SIMON WALDEMAR PRIPP
FRODE KVALNES

SUPERVISORS

Magnus Mikael Hellström

Martin Marie Hubert Choux

University of Agder, 2023

Faculty of Engineering and Science

Acknowledgements

Frode Kvalnes

Grimstad, Norway

Simon W. Pripp

Grimstad, Norway

May 19, 2023

i

Abstract

The use of lithium-ion batteries (LIBs) has rapidly increased recent years, mainly due to the global adoption of electric vehicles (EVs). Continued growth is expected, which will inevitably lead to a large amount of battery waste. Proper recycling is then required to reinsert valuable raw materials to the value chain. Recycling of LIBs are normally initiated by disassembly, followed by various mechanical and metallurgical treatments. Disassembly is one of the most labour intensive steps when recycling LIBs. Considering the expected growth, a fully automated disassembly process will be required. However, this represents a non-negligible investment.

Determining the optimal disassembly level prior to recycling is a crucial step that must be considered before investing in automated disassembly. Currently, most EV LIBs are only disassembled to module level prior to recycling. Instead, disassembly to cell level could produce greater purity material streams and less material to handle downstream. The question is whether or not it is economic viable to carry out deeper robotic disassembly down to cell level instead of stopping at module level. This study presents a techno-economic assessment of a robotic module disassembly line, furnishing guidelines on the necessary degree of automation in EV LIB disassembly. Different case study scenarios are proposed, demonstrating that investments in a robotic module disassembly line could be profitable.

Contents

List of Figures

List of Tables

Nomenclature

Abbreviations

AI   Artificial Intelligence

CE   Circular Economy

CMC Cell Management Controller

CO2 Carbon Dioxide

EoL   End-of-Life

EV   Electric Vehicle

GHG Greenhouse Gas

LCO Lithium Cobalt Oxide

LFP   Lithium Iron Phosphate

LIB   Lithium-ion battery

NCA Nickel Cobalt Aluminium Oxide

NMC Lithium Manganese Cobalt Oxide

NPV Net Present Value

PHEV Plug in Hybrid Electric Vehicle

SoH   State-of-Health

UiA   University of Agder

WEEE Waste from Electrical and Electronic Equipment

List of symbols

σ Standard deviation

σ^2 Variance

σ_{total} Expected duration of disassembly process

σ_{total} Sum standard deviation

C_a Annual costs

C_c Capital cost

C_e Cost of electricity

C_i Investment cost

C_m Cost of maintenance

C_s Cost of software

CF Cash flow

E Expected value

i Index for each equipment

m Most likely estimate

M_{mz} Mass of module material z

$Mtot_{mz}$ Total mass of module material

n Service lifetime

o Optimistic estimate

p Pessimistic estimate

P_i Power consumption of hardware

Q Annual troughput

r_d Discount rate

R_m Revenue from module materials

t_i Working time of equipment

V_{mz} Value of module material z

X_i Expected activity duration

z Index for each material

Chapter 1

Introduction

1.1 Background

The global temperatures are rising, making climate change a global emergency that can only be solved by international cooperation and coordinated solutions (United Nations, n.d.). As a response, the Paris Climate Agreement was signed by world leaders in 2015. The agreement is set to secure commitment from all involved countries to lower their emissions, aimed at limiting the increase of global temperature to 1.5 ℃ above pre-industrial levels compared to the current trend of 3 ℃ (Crooks, 2020; UNFCCC, n.d.). In 2020, the European Commission presented an updated plan on how to reach the objectives set in the 2015 agreement. The main objective was a 55% reduction of global climate gas emissions within 2030, compared to 1990-levels. Within this context, the transportation sector stands as the predominant contributor to greenhouse gas (GHG) emissions, encompassing 28% of global GHG emissions in 2021 (US EPA, 2023). In light of this, policy measures pertaining to renewable energy and CO_2 emissions regulations for vehicles has emerged as crucial initiatives proposed to attain the established objectives of the European Commission (n.d.). Actions like these, combined with many European governments' increased subsidy schemes for Electric Vehicles (EVs), have significantly boosted the electrification of transportation and rapidly increased the global adoption of EVs (International Energy Agency, 2021).

In 2020, the global EV stock reached 10 million, a 43% increase from 2019 (International Energy Agency, 2021). In the same year, EVs saved more than 50 Mt CO_2 equivalent of greenhouse gas emissions globally, equalling the emissions from the energy sector in Hungary in 2019 (International Energy Agency, 2021). The global sales of EVs are expected to increase to 30 million in 2030, compared to 3 million in 2020 (Alfaro-Algaba & Ramirez, 2020). The increasing use of EVs causes a growing demand for Lithium-Ion Batteries (LIBs), since the

majority of EVs are equipped with or powered directly by LIBs (Chen et al., 2019). Battery demand worldwide grew by 30% annually from 2010 to 2018, reaching a volume of 180 GWh in 2018 (International Energy Agency, 2021). Continued growth is expected at an 25% annual rate, reaching a volume of 2,600 GWh in 2030. By 2030, electric mobility will account for 89% of the global battery demand (World Economic Forum, 2019). Consequently, a large number of LIBs are expected to reach their End-of-Life (EoL) stage in the coming years. Statista's statistical analysis projects that the number of EoL EV batteries available for recycling in the European Union will rise significantly from 97,520 in 2023 to 1,103,764 by 2030 (Statista, 2023). At the same time, the resources in critical raw materials (e.g. cobalt, lithium and nickel) for LIB production are limited. Therefore, recycling of EoL LIBs to recover valuable raw materials and reduce the amount of Waste from Electrical and Electronic Equipment (WEEE) is critical.

In 2020, the European Commission established new requirements and targets regarding recycled materials and collection, treatment and recycling of batteries at EoL, proposing a circular economy for battery value chain (European Comission, 2022). By 2030, all industrial, automotive and electric vehicle batteries have to be collected and recycled in full, while achieving high levels of recovery (European Comission, 2022). Recovery of materials such as cobalt, lithium and nickel are emphasized in particular. Current LIB recycling processes can only divert some of the expected waste streams of spent EV batteries (Harper et al., 2019). However, further advancements are imperative to fulfill the requirements established by the European Union with regard to the capacity of the recycling industry, material purity, and recycling efficiency (Brückner et al., 2020).

At present, there exists a considerable amount of techniques employed for recycling LIBs. Broadly, these can be split into three main processes: pyrometallurgy, hydrometallurgy and direct recycling. These processes are covered in depth in a number of recent articles (Brückner et al., 2020; Chen et al., 2019; Harper et al., 2019; Or et al., 2020; Sommerville et al., 2020; Wei et al., 2023; Zhao et al., 2021). Prior to recycling, most EV batteries are disassembled to module level before being subjected to shredding (e.g. size reduction) followed by various sieving techniques (Harper et al., 2019). At the present time, most EV batteries are manually disassembled. This is mainly due to relatively low volume waste streams and several product variants making automation a major challenge (Harper et al., 2019; Thompson et al., 2020). Moreover, EV batteries are complex structures designed to provide rigidity and longevity throughout their operation, utilizing hermetically sealed

cells connected by a variety of joining techniques (glue, welding, mechanical joining) (Chen et al., 2019; Thompson et al., 2020). Put differently, EV batteries are not designed with disassembly in mind. For this reason, manual disassembly is a complex process, characterized as labour-intensive and costly while requiring highly trained personnel due to high voltage hazards (Choux et al., 2021; Thompson et al., 2020). Based on these factors, when the volumes of spent LIBs increases, manual disassembly will represent a major bottleneck in recycling (Glöser-Chahoud et al., 2021).

With the expected volume increase, a more autonomous process for LIB recycling will be required. A proposed solution in the literature is to apply robotics and artificial intelligence to automate the disassembly process. This could potentially erase several of the challenges related to manual disassembly (Harper et al., 2019). Although robotic disassembly of EV LIBs is a serious challenge due to many product variants and insufficient battery labeling, automation is an active research area with advancing progress (Choux et al., 2021; Li et al., 2018; Marshall et al., 2020; Marturi et al., 2018; Poschmann et al., 2021). Additionally, there is a significant amount of active research on EV LIB recycling, as well as various research projects. Research projects such as Lithium ion Battery Recycling (LIBRES) (NFR: LIBRES - 282328) and Lithium ion BATteries - Norwegian opportunities within sustainable end-of-life MANagement, reuse and new material streams (BATMAN) (NFR: BATMAN: 299334) have lately involved the University of Agder (UiA). Currently, UiA is one of the consortium members of the 2022 European Union funded RHINOCEROS project (EU: RHINOCEROS - 101069685). The project aims at "[. . .] develop, improve and demonstrate, in an industrially relevant environment, an economically and environmentally viable route for re-using, re-purposing, re-conditioning and recycling of EoL EV and stationary batteries" (Rhinoceros, n.d.). One of the projects main objective, assigned to UiA, is to develop a smart sorting and dismantling system enabling automated classification and dismantling of LIBs. This include an automated characterization of battery state, discharge via the grid and automated dismantling for reuse or recycling. This master's thesis does not contribute to the Rhinoceros project, but is strongly motivated by UiA's tasks and responsibilities in the project.

1.2   Problem formulation

One of UiA's contributions to the Rhinoceros project includes automated disassembly. To complete this task, a decision must be made on the optimal level of disassembly for an EV battery pack destined for recycling. Until now, UiA has focused on automated disassembly from pack to module level. A decision must be made on whether to stop at this level, or to proceed to cell level.

As earlier mentioned, most EV LIBs are disassembled to module level at least prior to recycling. While this can be effective for partial recovery of some materials, some argue that shredding of modules produce impure, mixed and contaminated waste streams, yielding a decreased recovery rate (Thompson et al., 2021; Marshall et al., 2020). An alternative would be to disassemble the module into cells, which provides less material to process during later stages of recycling, while potentially producing greater purity waste streams. For example, in the mechanical processing of shredded material (e.g. separation of steel components), it might be possible to save some steps if no steel components is present (assuming the cells have no steel). This could potentially result in cost savings. Furthermore, greater purity waste streams, obtained by shredding cells instead of modules, could potentially increase the recycling efficiency and purity of output materials, thereby increasing recycling revenue (Thompson et al., 2021). Also, because the cells are smaller in size than the modules, volumetric benefits may be obtained, potentially increasing recycling income, given that the cells contains the most valuable materials.

These things considered, the purpose of this master's thesis is to perform a techno-economic assessment of automated disassembly for recycling from module to cell level. In other words, the economic viability of a robotic module disassembly line will be assessed on the condition that processing (e.g. shredding) of battery cells instead of battery modules influences recycling revenue. With this intention, the findings from this thesis should enable UiA to make an adequate decision on whether or not to stop automated disassembly at module level. The analysis will include a comparison of three commercially available EV battery modules.

The literature contains a wide range of contemporary techno-economic research on LIB recycling, disassembly, and disassembly planning. Alfaro-Algaba and Ramirez (2020) studied the optimal disassembly level for EV LIBs, concluding that disassembly might be stopped at partial disassembly depending on the State of Health (SoH) of the battery modules. However, the study did not examine recycling as an option for the recovered modules. Rather, reuse of

modules at a good SoH was explored. Moreover, the study was based on manual disassembly to module level, with no consideration of disassembly to cell level or automation of the disassembly process.

Thompson et al. (2021) performed a techno-economic assessment of LIB recycling, comparing shredded material vs disassembled cells as input to the recycling process. Ten different hydrometallurgical processes was contrasted, whereas five used shredding of cells and the rest used disassembled cells as input. The study shows that disassembly instead of shredding could potentially provide significant cost savings, arguing that shredding delivers lower purity products and decreases process economics. The authors concluded that shredded material can be recycled into new cathode material with a cost saving of up to 20% while disassembled cells enable cost savings of up to 80%. Important to realize, the study did not account for the costs of disassembling the cells. It should be recognized that disassembly of battery cells is more complex compared to disassembly of battery modules (Alfaro-Algaba & Ramirez, 2020). In essence, while concluding that disassembled cells enables significant cost savings, automation of this step has received little attention in the literature and is not expected in near future.

Lander et al. (2023) present a comprehensive, techno-economic study on the cost of disassembly on various EV battery pack designs from pack level down to cell level. Three scenarios were developed, including a purely manual disassembly process, a semi-automated process and a fully-automated process. The results shows that a fully-automated process decreases the labour costs by 97% per pack while increasing the annual disassembly capacity by 600%. While this is true, factors as cell chemistry, recycling cost and revenue generated from recovered materials are out of the scope of the analysis. The study exclusively analyses the cost of disassembly.

As can be seen from the existing literature on similar topics, there is currently an important knowledge gap on whether automated disassembly should stop at module or cell level prior to recycling. Alfaro-Algaba and Ramirez (2020) considers the option of reuse. However, recycling is the ultimate fate of all EoL EV LIBs (Thompson et al., 2021). Thompson et al. (2021) argues that disassembled cells produce higher purity waste streams in comparison to shredded modules. Although this might be true, automation of such a high level of disassembly is not expected in near future considering that automation from module to cell level is yet to be proven on an industrial scale. Finally, as Lander et al. (2023) proved, automated

disassembly to cell level reduces disassembly costs compared to manual disassembly. However, the study does not prove whether or not disassembly to cell level is necessary from a recycling point of view. Hence, this thesis project will address those shortcomings of previous studies in the area.

1.2.1 Scope of research and research question

In connection with the Rhinoceros project, UiA has until now focused on automated disassembly to module level. Therefore, the scope of research in this thesis is limited to automated disassembly from module level to cell level, not pack to cell level. Furthermore, while the Rhinoceros project considers reuse, repurposing, reconditioning and recycling of EoL EV batteries, this thesis exclusively analyses the recycling option, as this is the ultimate fate of all EoL EV LIBs. Equally important, this thesis acknowledges that recycling can be performed through various processes, such as hydrometallurgy, pyrometallurgy, or direct recycling. However, it solely focuses on hydrometallurgy as it is expected to become the primary recycling method in the future, as stated by Thompson et al. (2021). Finally, understanding the economic factors of automated module disassembly is crucial to the scope of this thesis. Given the discussion above, the following research question are formulated:

RQ: Is it economically viable to invest in a robotic module disassembly line from a recycling perspective?

1.2.2 Thesis Structure

This thesis is organized as follows. Chapter 2 presents relevant theory on technical and economic aspects of EV LIB batteries, disassembly and recycling. Chapter 3 is dedicated to presenting the methodology for assessing robotic module disassembly and modelling a recycling process. Results on cost of disassembly and potential recycling revenues are presented in chapter 4 and then the significance of the results are discussed in chapter 5. Finally, chapter 6 summarizes the main findings of the study, reviews its limitations, and suggests avenues for future research.

Chapter 2

Theory

To address the research gap identified in Section 1.2, a understanding of relevant theoretical background is important. This chapter presents relevant technical and economic background on EV LIB batteries, disassembly and recycling. First, key concepts concerning circular economy with respect to batteries are presented in Section 2.1. Following, Section 2.2 presents a fundamental understanding of the LIB, including its alternative pathways once it has been decommissioned from the vehicle. Subsequently, theoretical background on LIB recycling is outlined in Section 2.3, covering the main stages of recycling: disassembly, mechanical processing and hydrometallurgical treatment. Additionally, this section covers the challenges faced in disassembly and recycling in general. Section 2.4 presents an elaboration on automated disassembly of LIBs, highlighting its potential benefits, challenges, and future prospects. Finally, Section 2.5 outlines on the use of techno-economic analysis as a method of analysing economic performance of industrial processes.

2.1 A circular economy for battery value chain

The Circular Economy (CE) builds on a general understanding that the Earth's resources and energy are limited, and that pollution and waste should be avoided. CE describes an economic system where resources are used, recycled and reused, minimizing waste and pollution in an efficient and sustainable manner (Stahel, 2016; Zhao et al., 2021). This approach facilitates the closing of loops in industrial ecosystems (Stahel, 2016). A circular battery value chain refers to an ideal sustainable process for creating and using batteries, where all activities are designed to be as sustainable and resource efficient as possible in order to maintain a closed loop of resources. The World Economic Forum's insight report highlights the significance of a circular battery value chain as a major factor in achieving the Paris Agreement's target of limiting global temperature (World Economic Forum, 2019).

For the battery and EV industry to appropriately adapt to such sustainable goals and ambitions of CE, governments and authorities are required to develop regulations for battery disposal after EoL, labelling of materials, collection rates, recycling efficiency, as well as minimum requirements for recovered materials used in new batteries (Ali et al., 2022; Or et al., 2020). In relation to this, the European Commission has launched a new Circular Economy Action Plan, COM (2020) 798: Proposal for a REGULATION OF THE EUROPEAN PARLIAMENT AND OF THE COUNCIL concerning batteries and waste batteries, repealing Directive 2006/66/EC and amending Regulation (EU) No 2019/1020, which succeeds the battery directive of 2006, and contributes to the existing framework on EoL vehicle directives from 2000 (European Commission, 2000, 2006, 2020. It is a regulatory framework that targets batteries and vehicles with the objective to reduce waste of rare earth materials and increase the duration resources are in the value chain.

The proposed directives target recycling efficiency on LIB to be 65% by 2025, and 70% by 2030. Additionally, individual material recovery rates for Co, Ni, and Cu is set to 95%, and 70% for Li by 2030 (European Commission, 2020). As of January 1st, 2030, the manufacturing of new batteries must meet to the following minimum requirements for incorporating recovered waste materials: Co at a rate of at least 12%, and Li and Ni at a minimum of 4% (European Commission, 2020). These values are set to increase to 20% for Co, 10% for Li, and 12% for Ni by January 1st, 2035 (European Commission, 2020). Furthermore, all waste originating from EV batteries is to be collected without cost for the last holder or the owner of the vehicle, regardless of brand, condition, and chemical composition (European Parliament, 2023).

2.1.1 Challenges with battery value chain

Adopting a circular economy model for a battery value chain could be difficult for an organisation. Financial concern was found in a study by Wrålsen et al. (2021) as the most recurring barrier that could prevent circular practices for spent LIBs. For example, Albertsen et al. (2021) argues that the integration of recycled materials into the supply chain could potentially lead to increased transportation expenses. Moreover, lack of standardised materials in the battery chemistry makes a circular value chain for LIBs difficult as the profitability from recovery becomes uncertain and volatile (Ahuja et al., 2020). Furthermore, while automating the disassembly process has the potential to decrease recycling costs, the financial viability of EV battery recycling and material recovery ultimately depends on the composition of the battery materials and the market value of the recovered elements (e.g. Co, Ni and Li)

(Lander et al., 2023). Additionally, technological advancements can make critical materials obsolete, and decreased prices for new LIBs may remove financial advantages for the recovery of materials (Martinez-Laserna et al., 2018). In this context, technological advancement refers to the development of new and improved materials, manufacturing processes, and battery chemistries that can lead to the replacement of current critical materials used in LIBs with new and alternative ones.

To facilitate closed loops within a circular economy, it is imperative for manufacturers to integrate circular economy considerations into the design process at the earliest stages (Bocken et al., 2016). In context of a battery value chain, EV manufacturers must employ design strategies that prioritize the realization of a circular material flow through products that are designed to be recycled.

2.2   The lithium-ion battery

The lithium-ion battery is characterized by high energy density, long lifetime, good charging/discharging efficiency, light weight and cycle stability (Alfaro-Algaba & Ramirez, 2020; Or et al., 2020). This makes it suitable as the main source of energy in an EV. The LIB consist of four main components: anode, cathode, electrolyte and separator (Alfaro-Algaba & Ramirez, 2020). The anode and cathode, also know as negative and positive electrode, respectively, are manufactured with lithium metal oxide and lithiated graphite (Hannan et al., 2018). The cathode material is the main vital component in LIBs given its major role in the electrochemical reactions taking place. The performance of this material directly affects the energy density, the durability in terms of cycle life, and the voltage at which it operates (Zhao et al., 2021). More detailed information of the LIB main components are covered by (Brückner et al., 2020).

During discharging, lithium-ions leave the anode and enters the cathode, and vice versa during charging. The electrolyte is made of lithium salts and organic solvents, enabling the transportation of lithium-ions between the anode and cathode (Hannan et al., 2018). The separator is a micro-porous membrane set to prevent short circuits between the anode and cathode, while only allowing lithium ions to pass (Hannan et al., 2018). An EV battery pack are normally composed of battery modules and a battery management system (Alfaro-Algaba & Ramirez, 2020). The modules are assembled from numerous of series-parallel connected battery cells.

The quantity and geometry of cells constituting a module varies depending on manufacturer. This is shown in Figure 2.1, where battery designs from three well established EV manufacturers are depicted. The Tesla Model S Mk1 85kWh Battery Pack consist of 16 modules per pack with 444 cylindrical cells per module. The Nissan Leaf Mk1 22kWh Battery Pack consist of 48 modules per pack with 4 pouch cells per module. while the BMW i3 Mk1 22kWh Battery Pack consist of 8 modules per pack with 12 prismatic cells per module.
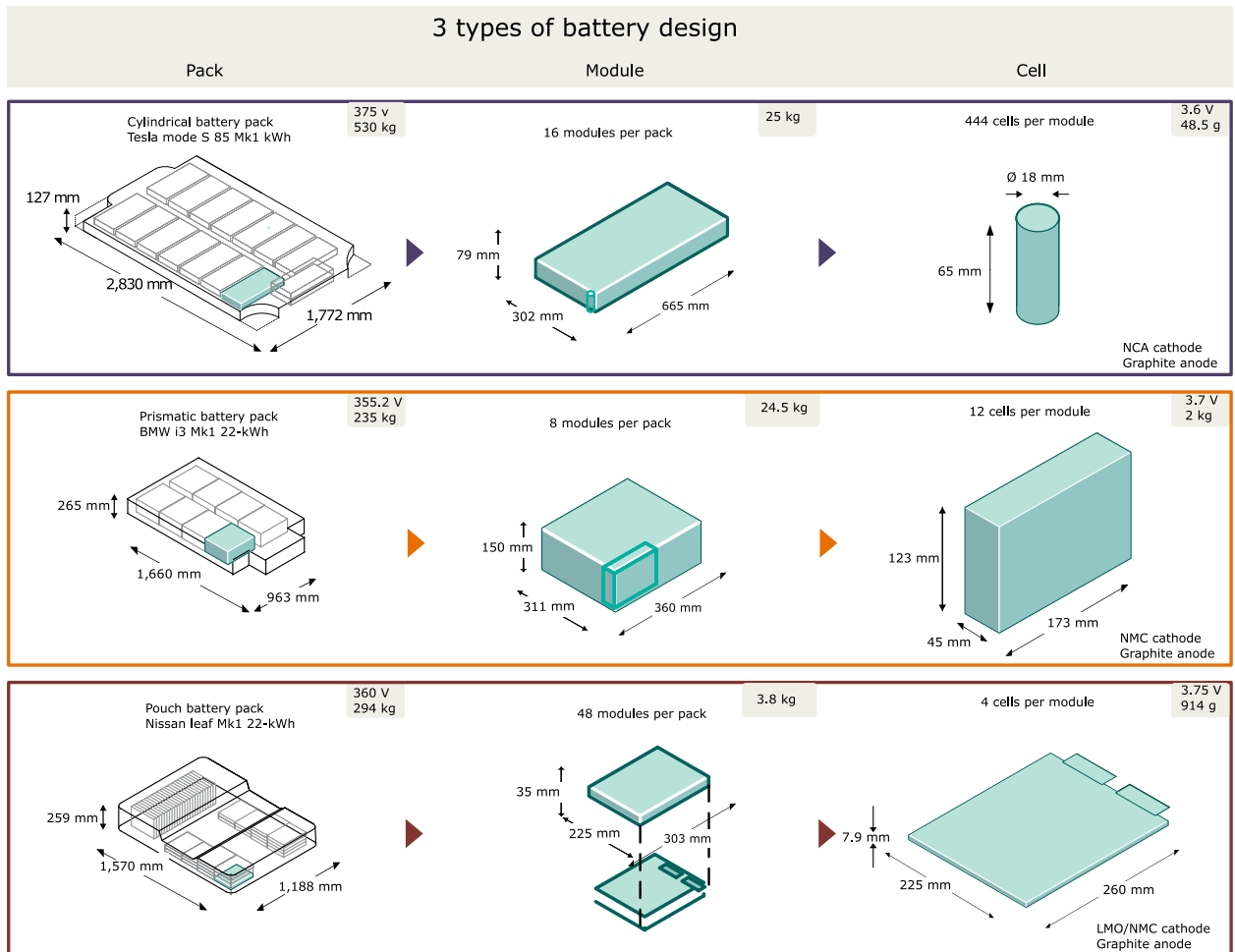
Figure 2.1: Different types of EV batteries (Reworked from Harper et al. (2019)
.

2.2.1 LIB technologies and chemistries

Battery manufacturers will always seek to develop batteries of improved performance at reduced costs. As a result, LIB chemistries and designs are prone to changes. The cathode have been developed with a variety of different chemistries: Lithium Cobalt Oxide (LCO), Nickel Cobalt Aluminium Oxide (NCA), Lithium Nickel Manganese Cobalt Oxide (NMC) and Lithium iron phosphate (LFP) (Alfaro-Algaba & Ramirez, 2020). Traditionally, LFP technology has captured the largest market share (He et al., 2017). However, NMC and NCA technologies are currently experiencing increased adoption due to their superior energy density and power capability (He et al., 2017; Zhao et al., 2021). While Tesla is utilizing NCA technology (He et al., 2017), NMC technology is currently the most widely adopted cathode chemistry in EV LIBs (Alfaro-Algaba & Ramirez, 2020; Hannan et al., 2018; Olivetti et al., 2017). Moreover, Zhao et al. (2021) refers to a study by Frost and Sullivan which forecasts that the share of NMC in global LIB production is expected to increase from 19% in 2018 to 48% in 2025. It is important to realize that there are multiple compositions in the NMC class (Olivetti et al., 2017). To mention some: NMC111 (containing 1 part Ni, 1 part Mn and 1 parts Co), NMC622, NMC811 and NMC9.5.5 (Element Energy, 2019; Olivetti et al., 2017). The most widely adopted composition is the NMC622 (containing 6 parts Ni, 2 parts Mn and 2 parts Co), which offers a low self-heating rate and high energy density (Alfaro-Algaba & Ramirez, 2020; Element Energy, 2019).

Forecasts shows that NMC811 will dominate the market by 2025 and NMC9.5.5 by 2030. This is coupled with the current trend of replacing expensive metals such as cobalt with higher amounts of cheaper substitute metals (e.g., Ni and Mn) in response to cost and availability-related concerns (Chen et al., 2019; Element Energy, 2019). Under such circumstances, the cobalt content will be reduced from 20% (NMC622) to 5% (NMC9.5.5) by 2030. This will have significant implications on the recycling industry, as existing business models depends largely on high-value cobalt recovery (Chen et al., 2019).

Bajolle et al. (2022) reported in a study based on interviews with industry experts that NMC technology is expected to dominate a significant portion of the market until at least 2030. Despite this projection, some experts contend that LFP technology may be a feasible option for certain countries, such as China and certain developing nations, owing to its low cost, as also pointed out by (Bajolle et al., 2022). On the other side, LFP technology offers less energy density and consequently shorter driving range. However, it compensates for the drawbacks by offering a longer life cycle, and are therefore often used in Plug-in Hybrid Electric Vehicles

(PHEV). Another discussion in the literature is the potentials of solid state batteries, which utilize solid electrodes and electrolytes instead of liquid or polymer gel electrolytes to provide higher energy density and faster charging times. Bajolle et al. (2022) concludes that this technology is unlikely to be seen at an industrial scale before 2030. Although alterations to LIB chemistries are ongoing, the primary focus of this study pertains to products that have already been introduced to the market because recycled materials in the near future will be derived from past market sales.

2.2.2 The lithium-ion battery value chain

A lithium-ion cell typically has a lifespan of between 500 to 3,000 charge/discharge cycles in its original application (Cicconi et al., 2012). The LIB is decommissioned from the vehicle and processed by a battery handler when the energy capacity drops by 20% to 30% compared to original capacity (Chen et al., 2019; Wrålsen et al., 2021). The options to properly handle spent LIBs include remanufacturing, repurposing and recycling. Remanufacturing and repurposing aims at extending the life of the battery, while recycling returns the batteries' critical materials to the value chain (Chen et al., 2019). From an environmental perspective, remanufacturing or repurposing first, followed by recycling would maximise the value of an LIB (Chen et al., 2019). Remanufacturing enables spent LIBs with acceptable SoH to be re-used in automotive applications. Normally, only a small share of cells fails to hold the required capacity when the energy storage capacity of an LIB decreases below 80%. Under these circumstances, replacing the out of tolerance cells makes the battery pack applicable to be re-used in its original application (Chen et al., 2019). However, only 5% of EoL LIBs are expected to be remanufactured in the long term due to the trend of homogeneous cell aging (Zhao et al., 2021). As the same level of deterioration would apply for all cells, replacing individual cells would be economically unfavourable.

Repurposing, often referred to as second use, involves utilizing spent EV batteries in secondary applications where the battery performance is less critical (Harper et al., 2019). Such secondary applications are normally stationary energy storage used for peak shaving, swapping power stations or load shifting (Harper et al., 2019; Chen et al., 2019). Repurposing for second use requires reconfiguration on battery pack, module or cell level, in addition to the integration of a new battery management system (Chen et al., 2019; Wrålsen et al., 2021). A second use battery is viable for a secondary application until it reaches 60% of original capacity (Cicconi et al., 2012). Below this limit of SoH, the significant voltage losses could compromise the battery safety.

Both remanufacturing and repurposing extend the LIB value chain by further exploiting the product over time. This could be beneficial from an environmental and economic perspective, depending on factors such as future market characteristics and battery degradation mechanisms (Wrålsen et al., 2021). Depending on application, the employment of a LIB for a second use application does introduce a lag of five to ten years before the critical raw materials are re-inserted to the battery supply chain via recycling (Thompson et al., 2020). According to Kamran et al. (2021), such a lag only marginally affects the demand for virgin materials, due to saturation of supply demand in the stationary energy storage sector. In other words, the future volume of spent LIBs are expected to exceed the quantity that the second use marked can absorb (Harper et al., 2019; Kamran et al., 2021; Zhao et al., 2021). Regardless of second-use or not, recycling is the ultimate fate for all LIBs. Recycling is covered in the next chapter, being the main focus of this thesis.

2.3   Lithium-ion battery recycling

Generally, there are two main routes to LIB recycling: the mechanical and the pyrometallurgical route. The latter route processes the batteries in a high-temperature metallurgical process with limited need for pre-treatment (Rouhi et al., 2021). The mechanical recycling route consists of two main processes: hydrometallurgical processing and direct recycling. These processes requires more pre-treatment, employing mechanical processing steps such as shredding and magnetic separation as preliminary steps (Ali et al., 2022; Sommerville et al., 2020). The three processes are displayed in Figure 2.2. It should be noted that some recycling companies uses a combination of the above mentioned recycling processes (Sommerville et al., 2021).

Before an EV battery can be mechanically processed, the battery must be disassembled, making disassembly an unavoidable step in the mechanical recycling route (Alfaro-Algaba & Ramirez, 2020). Effective disassembly prior to recycling could optimize output fractions and reduce negative environmental effects (Schwarz et al., 2018). Since disassembly is a crucial aspect of this thesis, this chapter will first provide an overview of the disassembly process for EV batteries.
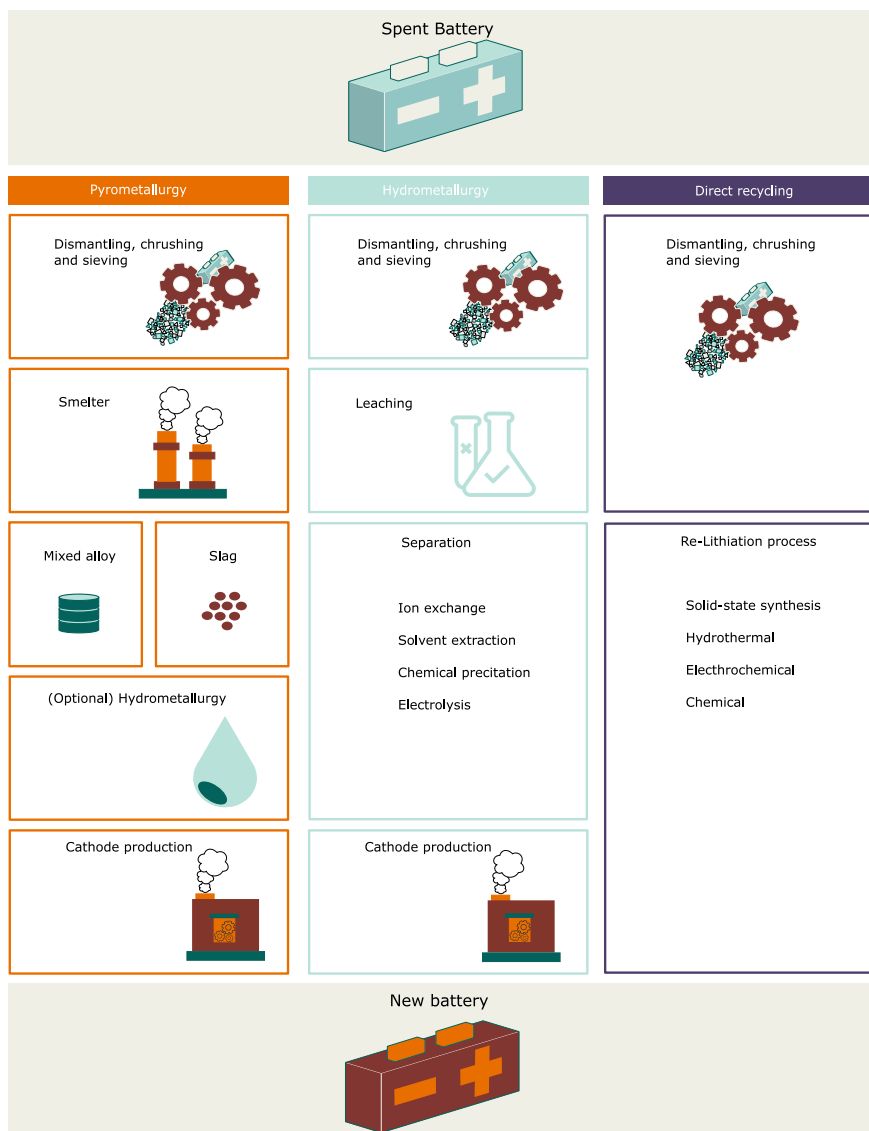
Figure 2.2: Different Recycling Techniques. (Reworked from Chen et al., 2019)

2.3.1   Manual disassembly of EV batteries

To mitigate the risk of high voltage hazards, the initial step in the disassembly process is to discharge the batteries (Wegener et al., 2015). The discharging process is covered in depth by Rouhi et al. (2021) and Sommerville et al. (2020). Following discharging, the batteries are typically disassembled to module level at least, although for some pyrometallurgical processes, discharging and high-level disassembly may be optional (Harper et al., 2019; Wegener et al., 2015).

As previously noted, there are several variations in EV battery designs, which differ not only among manufacturers but also among different models of the same car (Wegener et al., 2015). This is partly due to the fact that most car manufacturers make limited modifications to their conventional cars to make them electrically powered (Wegener et al., 2015). As a result, the battery is often sized to fit into an existing car body. Nevertheless, some basic steps for

disassembling an EV battery are outlined in Table 2.1. Note that step VI is optional and investigated further in this thesis.

Table 2.1: Generic disassembly steps, of Wegener et al. (2015)

Step	Description
I	Opening of the battery system, i.e. removal of the cover
II	Cutting of the electrical connections between the battery modules and the electronic components
III	Removal of the mechanical connections between the system components and the battery base
IV	Removal of the electronic components
V	Removal of the battery modules
VI	*Disassembly of the battery modules and removal of the battery cells*

Currently, most EV batteries are manually disassembled with limited degree of automation (Choux et al., 2021; Wegener et al., 2015). The lack of automation is primarily due to the current low volume of EoL LIBs, the presence of several design variations, and a lack of detailed designs of the batteries that are available to the recycler (Glöser-Chahoud et al., 2021; Wegener et al., 2015). A discussion on the automation of the disassembly process is presented in Section 2.4.

2.3.2 Challenges of disassembly and safety considerations

Manual disassembly processes are complex and labour-intensive, consuming time and costs while requiring highly skilled personnel (Choux et al., 2021). Schwarz et al. (2018) argues that disassembly is one of the most expensive step in the recycling process. Likewise, Lander et al. (2021) found that the disassembly cost contributed from 15% to 20% to the total recycling costs in the UK and Belgium. Consequently, complete manual disassembly of an EV battery might not be economic viable and therefore stopped at an optimal level (i.e. partial disassembly) (Alfaro-Algaba & Ramirez, 2020; Choux et al., 2021).

One of the largest barriers to efficient disassembly is the way in which the cells, modules and packs are assembled (Thompson et al., 2020). The cells are normally hermetically sealed, whereas the modules and packs are glued together. While this provides rigidity, safety and cell longevity, it reduces the recycling efficiency (Thompson et al., 2020). Furthermore, the variety of physical configurations, cell types and cell chemistry's promotes the need for different disassembly approaches and metals reclamation, affecting the overall economics of recycling (Harper et al., 2019; Thompson et al., 2020). Lander et al. (2023) studied the impact of battery pack design on disassembly costs, and found that the disassembly costs

per disassembled kWh could vary by 84% between different battery pack designs, ranging from \$4.07/kWh (Nissan Leaf) to \$0.62/kWh (BYD). The cost variation was mainly due to the significant differences in number of modules and fasteners.

Apart from barriers stemming from assembly, manual disassembly impose several safety concerns. The process requires high-voltage training and specialized insulated tools to obstruct electrocution of operators or short circuiting of the pack (Harper et al., 2019). High amounts of residual power in the cells makes them vulnerable to toxic gaseous emissions, explosions and fires (Ahuja et al., 2020). Ali et al. (2022) reported that 90% of fires at German recycling facilities are caused by LIBs. Another concern is the shortage of trained technicians capable of handling EVs. A survey by the Institute of the Motor Industry, referred to by Harper et al. (2019), found that 1,000 technicians where trained to handle EVs in the UK, only representing 2% of the total workforce of motor technicians.

In general, manual disassembly is expected to represent a substantial bottleneck in the EoL battery treatment as the volume of spent LIBs continue to increase (Glöser-Chahoud et al., 2021). Thompson et al. (2020) even argues that since the process is slow and costly, the only viable route to recycling becomes pyrometallurgy (requiring limited pre-processing), which on the other hand is expensive and inefficient. Some well established barriers to disassembly regarding pack removal, pack disassembly, module removal and cell separation is displayed in Figure 2.3.

Challenges of disassembly at different stages

Recovered components /materials	Disassembly step	Disassembly problems
	Spent EV	• Variety of vehicle shapes and sizes • Different pack configurations and locations • Different fixings and tooling required • Bolts and fixings may be rusted • Heads of fixings may be rounded or sheared • Position of bolt heads not always fixed • Vehicle bodywork may be distorted • Vehicle may be crash damaged • Weight of battery
• Bus bars • Electronics • Wiring looms • Modules > Cells • Other components	Pack	• Removal of wiring looms tricky • Manipulation of connectors (especially where locking tabs fitted) • High voltages until wiring loom/module links removed • Lack of data on module condition in many electric-vehicle batteries • Lack of labelling and identifying marks • Potential fire hazards • Potential offgassing of HF
• Casings • Terminals • Cells	Module	• Sealants may be used in module manufacture (difficult to remove) • Cells stuck together in modules with adhesives (difficult to separate) • Components may be soldered together (difficult to separate) • Module state of charge may not be known
(Depending on cell chemistry and recycling process) • Cobalt • Nickel • Lithium • Graphite • Manganese • Aluminium • Plastics	Cell	• Clean separation of anodes and cathode for direct recycling difficult • Very finely powdered materials present risks (nanoparticles) • Potential for HF compounds formed from electrolyte • Potential for thermal effects if cells shorted during disassembly • Chemistries not always known or may be proprietary • Additional challenges with cylindrical cells (unwinding spiral)
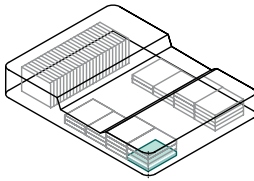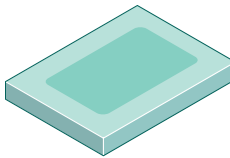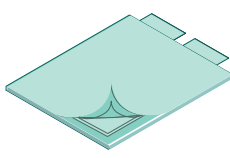
Figure 2.3: Challenges of disassembly at different levels of scale. (Reworked from Harper et al., 2019)

2.3.3 Mechanical processing

Following disassembly, the battery material is mechanically processed to separate the materials in different fractions. The LithoRec process could be utilized to provide insight to such mechanical processing steps (LithoRec II – Recycling of Lithium-Ion Batteries). The LithoRec II project, funded by the German Federal Ministry of the Environment in 2012, aimed at developing a new recycling process for EV LIBs combining mechanical, mild thermal and hydrometallurgical treatment. A process flow chart of the mechanical processing steps of LithoRec is presented in Figure 2.4. A detailed description of the different steps are described by Kwade and Diekmann (2017). A summary of the process steps follows.

First, the batteries are discharged and short circuited to enable safe disassembly and crushing. The batteries are then manually disassembled to module level before undergoing shredding under an inert atmosphere. The following step aims at removing the electrolyte and conducting salts covering the shredded material. For this step, LithoRec has proposed three possible process routes: solvent extraction, thermal drying or the use of supercritical CO_2. The next steps combines air-sifting, crushing and sieving processes to separate the different shredded materials. A magnetic separator is used to recover steel and most of the non-magnetic heavyweight fragments. Light weight fragments, consisting of the battery cell separator, current collector coils, plastic foils and coating materials, are separated by air-classification and further processed. A second crushing step is implemented after the magnetic separation step, exerting a cutting stress on the fragments. Consequently, separation of light weight fragments in a zig-zag sifter (e.g. density separator) is possible as the light weight fragments has increased their density due to the applied cutting stress. Finally, a vibration sifter is used to recover the active material and mixed plastic (e.g. separator) prior to optical separation of copper and aluminium. The active material (e.g. black mass) requires further hydrometallurgical processing to recover the cathode materials (Co, Ni, Li, Mn).
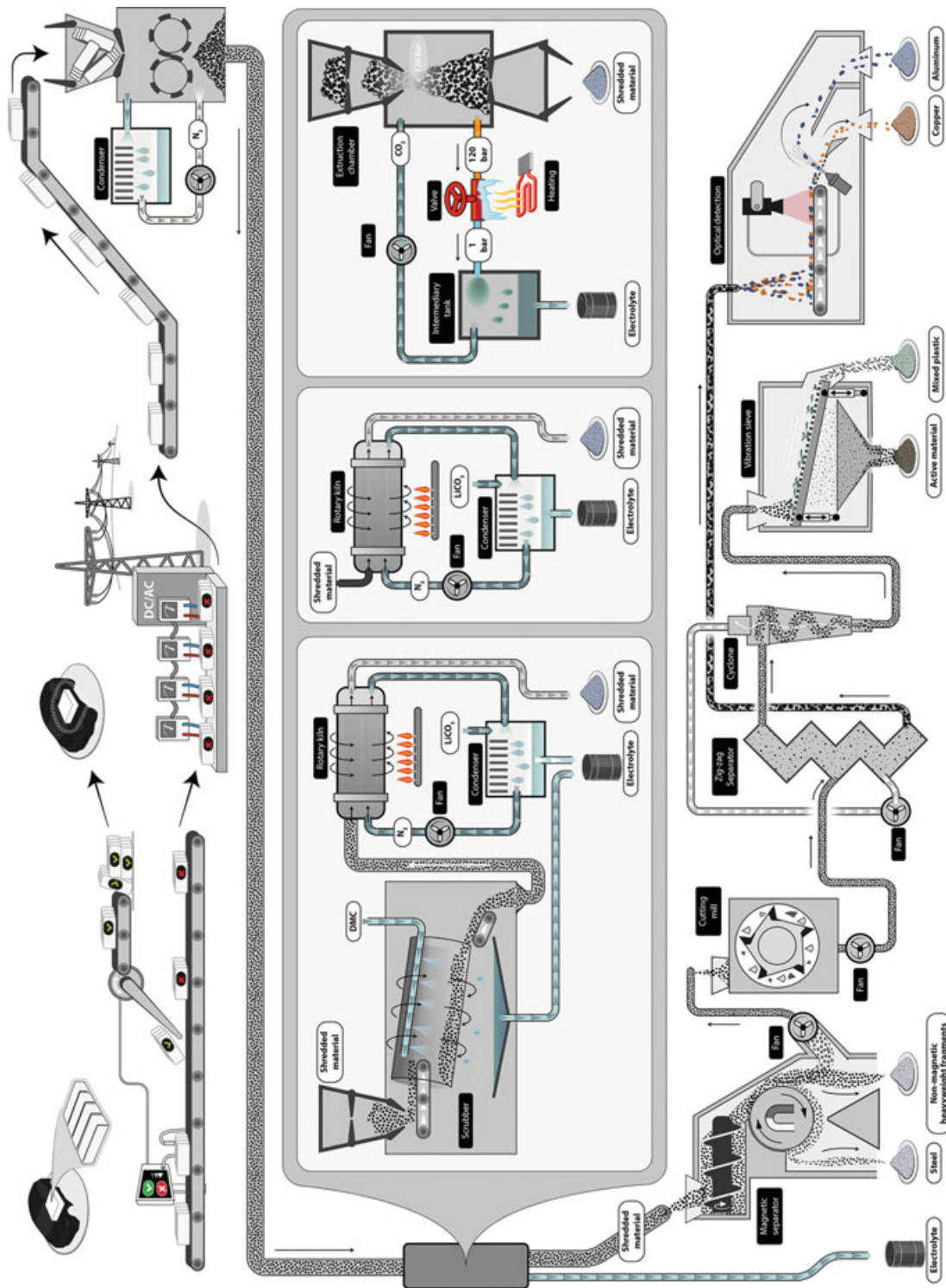
Figure 2.4: Process flow chart illustrating the mechanical process employed by LithoRec. Figure obtained from Kwade and Diekmann (2017)

2.3.4 Hydrometallurgical processing

Subsequent to the mechanical processing stages, the active material proceeds through hydrometallurgical processing to segregate the cathode materials. Hydrometallurgical processing is a technique that employs aqueous chemistry at low temperatures to extract metals from cathode materials (Brückner et al., 2020; Harper et al., 2019; Thompson et al., 2020). When physical separation is complete, a numerous of leaching techniques are being applied, including acid leaching, alkali leaching and bioleaching (Wei et al., 2023). After the leaching process, the metals are transferred into the leaching solution for the purpose of metal element recovery. Techniques used in this step are, among others, solvent extraction, chemical precipitation and electrochemical deposition (Wei et al., 2023). Hydrometallurgy enables the recovery of lithium, graphite, manganese and aluminium as metal extraction occurs in the first phase (Thompson et al., 2021). This reflects a process of greater yield than pyrometallurgy in terms of both quality and quantity of recovered materials. Xiong et al. (2020) states that hydrometallurgy could yield recovery rates of up to 98% for Cobalt and Nickel. Also, lower energy consumption and fewer CO_2 emissions are obtained during the low temperature operation (Ali et al., 2022; Thompson et al., 2020; Zhao et al., 2021). The main drawback of hydrometallurgy is the large number of process steps prior to metals reclamation which adds to the process complexity, such as pre-treatment involving disassembly and sorting based on cathode chemistry (Ali et al., 2022; Zhao et al., 2021).

2.3.5 Recycling process and economic challenges

There are a large number of research articles which reviews LIB recycling from different perspectives. A common theme in the articles is that there are many challenges that the LIB recycling industry must dissolve: automation of disassembly, safety considerations, improved sorting technologies and design for recycling (e.g. standardization) (Harper et al., 2019). Challenges regarding disassembly, design and safety have already been addressed in Section 2.3.2. This section cover challenges regarding the recycling process in general.

Insufficient battery labelling is a common issue in the LIB recycling industry. Unlike batteries used in internal combustion engine vehicles which are made of uniform and standardized chemistry's, the lithium-ion is more a common denominator for several different chemistry's based on the same principles (Ahuja et al., 2020). Therefore, recyclers need to sort batteries by chemical composition prior to the recycling process. However, most LIBs have no information regarding chemistry of the anode, cathode or electrolyte (Thompson et al., 2020),

making sorting a time consuming and labour-intensive process (Zhao et al., 2021). Ideally, the sorting process should be automated with robots as such technology is present (Harper et al., 2019). However, the lack of labelling makes this problematic. A potential solution called-upon is a battery passport, making the sorting and identification process much easier (Zhao et al., 2021).

A common economic concern in the recycling industry is the decreasing value of cobalt in the recent years. The economic viability of many recycling processes depends largely on cobalt recovery (Chen et al., 2019; Harper et al., 2019). Continued price drop of cobalt could make battery manufacturers choose virgin over recycled cobalt (Zhao et al., 2021). Consequently, recyclers would struggle to make profits. Moreover, as earlier mentioned, a current trend is present towards lower cobalt content in LIBs (Chen et al., 2019; Harper et al., 2019; Sommerville et al., 2021). This could make the future recycling industry less profitable given current circumstances (Zhao et al., 2021). It is therefore critical to develop flexible and improved recycling techniques, extracting as much material value as possible at reduced costs.

In general, the financial viability of current recycling techniques depends on several variables. The literature is conflicting while discussing the economic situation of recycling. Chen et al. (2019) argues that current recycling processes does not provide an economic solution to the increasing input streams of spent LIBs. In like manner, arguments are made that the recycling industry needs subsidies or gate fees to make recycling economic viable (Batteries Europe, 2020). On the other hand, it is believed that LIB recycling is profitable while using current techniques (Kachate et al., 2022; Lander et al., 2023; Thompson et al., 2020). Lander et al. (2023) found in their study that the net recycling profit could range from -21.43 to 21.91 dollar per kWh recycled depending on transportation and labour costs, pack design and recycling technique. The highest net profit was obtained by recycling a Tesla Model S battery pack using the direct recycling process in China, where labour costs are low. The study concludes that high net recycling profits is achieved via: recycling in countries with low labour costs, reducing transportation costs, economies of scale, high value battery chemistry recycling, direct instead of pyrometallurgical recycling and emphasis on design to disassemble. Currently, direct recycling is at lab-scale and at an early development stage, making profits of 21.91 dollar difficult to achieve in large-scale. Although this may be true, Lander et al. (2023) found that hydrometallurgical processes could yield net profits of up to 10 dollar per kWh. Again, such profits were achieved in China with low labour costs. In

Europe (Belgium and UK), only small profits ($2-3) were accomplished mainly due to higher labour costs.

2.4   Automated disassembly

As previously indicated, improved recycling technologies are required to accommodate the future volumes of spent LIBs. While discovering innovative processes is critical, improvements can be done to existing processes. For example, a cost-effective hydrometallurgical process is attainable on the condition that a minimum of extraneous material is subjected to the process (Sommerville et al., 2021). By the same token, shredding of battery modules could result in contaminated material streams and passivisation of reactive components, delivering lower purity products (Thompson et al., 2021). Ensuring high product purity is critical for LIB recycling since even minor contamination can render the final product unusable for EV batteries (Thompson et al., 2021). With this in mind, the implementation of robotic battery disassembly could potentially enhance the economic viability of recycling by improving the mechanical separation of materials and components (Harper et al., 2019). This can generate greater purity material streams while eliminating the high labour costs and bottleneck obstacles associated with manual disassembly (Harper et al., 2019). Equally important, automation could significantly reduce human work safety risks, as stated by Glöser-Chahoud et al. (2021).

That being said, robotic battery disassembly presents considerable challenges (Harper et al., 2019; Meng et al., 2022). So far, a materialized automated disassembly process from battery pack to cell level is yet to be proved in the literature. However, some literature has covered automatic disassembly of specific disassembly steps (Choux et al., 2021; Li et al., 2018; Marshall et al., 2020). These processes typically involves disassembly from pack level to module level, or module level to cell level. Additionally, disassembly using a hybrid human robot workstation is covered by Kay et al. (2022), Wegener et al. (2014) and Wegener et al. (2015), where the robots carry out simple tasks with human assistance.

While the works of Thompson et al. (2020) and Schäfer et al. (2020) have concluded that implementing design for disassembly and increasing the level of standardization in design can potentially address some of the challenges that are commonly associated with robotic disassembly, rapid changes to module and pack design appear due to technological advancements (Choux et al., 2021). In other words, standardization of design of LIB battery systems are improbable to happen in the near future (Harper et al., 2019).Therefore, research on ar-

tificial intelligence and development of new robotic technology with cognitive capabilities is by some viewed as an convenient solution (Choux et al., 2021; Zhao et al., 2021). The end goal of such a solution is that robotic disassembly is attainable without comprehensive prior knowledge of the product to disassemble. The following subsections is set to cover the current technological advancements and the major challenges in robotic disassembly.

2.4.1 Challenges in robotic disassembly

Automated disassembly of EoL electrical products has been implemented in different sectors (Harper et al., 2019). One example is Apple, which has implemented an automated disassembly line for the iPhone 6, dismantling 1.2 million phones per year (Harper et al., 2019). The disassembly line uses 29 robots to disassemble the phone into 8 discrete parts in 11 seconds. It must be remembered that the robotic environment at Apple is highly structured, where disassembly is a repetitive process based on pre-programmed robots handling the exact same model, unable to adapt to new models and varieties of phones. In contrast, considering the design variations of EV batteries, robotic disassembly of these is far more complex. The robots must be flexible and adaptable, handling a variety of objects and uncertainties in used EV LIBs, which is significantly different from pre-programmed repetitive tasks.

From this, one could argue that design variations is one of the main challenges in robotic disassembly (Choux et al., 2021; Harper et al., 2019; Meng et al., 2022). As mentioned earlier, standardized battery design is not expected in the near future. For this reason, a single robotic disassembly line must be able to handle a high variety of designs. Also, uncertain battery conditions represents challenges as spent LIBs may have significant differences in their physical conditions, such as rusted or defect components, stained surfaces and changed geometry (Meng et al., 2022). Moreover, the way in which the battery is assembled impose problems for robotic manipulation. Especially, flexible cables and fasteners difficult to access is troublesome. Meng et al. (2022) also argues that the lack of life-cycle data represent a challenge. This is coupled with the absent of battery labelling making it difficult to design an automated disassembly plan without information on cell compositions and the cells SoH. In short, most of the previously mentioned challenges in manual disassembly also applies for robotic disassembly and are well summarized in Figure 2.3.

2.4.2 Robotics and artificial intelligence (AI)

Automated disassembly of LIBs is an active research field that involves intelligent pre-processing of LIBs, intelligent disassembly planning and decision-making, and intelligent

disassembly operation (Meng et al., 2022). Intelligent pre-processing involves checking, test-ing and sorting spent LIBs to classify chemical composition and evaluate condition and quality (Meng et al., 2022). Intelligent disassembly planning and decision-making must han-dle the disassembly uncertainties, requiring cognitive capabilities to determine, for example, disassembly depth and optimal disassembly sequence (Meng et al., 2022). Intelligent disas-sembly operation involves target detection processes and the actual robotic disassembly of the LIB (Meng et al., 2022). To this date, AI is used for computer vision (i.e., target de-tection) and not for robotics concerning disassembly planning and the disassembly process. From the three above mentioned research fields, intelligent disassembly operation is most relevant for this study and are outlined further. Intelligent pre-processing and disassembly planning are covered in depth by Meng et al. (2022).

The variety of battery designs and lack of battery labelling makes intelligent target detection an inevitable step in robotic disassembly. In short, such a process should map the batteries screws, cables, modules and other components using computer vision (Meng et al., 2022). Typically, this involves capturing a series of 2D and 3D images of the battery, detecting the location of components and their respective coordinates, and storing this information for subsequent use. Once the images are processed and the various components are detected, the disassembly process can be initiated. A robotic disassembly system requires a tool-changing system that can quickly switch between different tools and sensors depending on the specific disassembly task (Meng et al., 2022). Force, torque, and tactile sensors such as fingertip force sensors are used to facilitate interaction between the robot and the battery (Harper et al., 2019; Meng et al., 2022). For example, a torque sensor can be utilized to determine successful interaction between a screw and the robots screwdriver, hindering screwdriver slippage (Meng et al., 2022). Furthermore, due to the presence of welded parts, operations such as cutting, milling, or drilling become necessary during the disassembly process.

Intelligent target detection and separation of various components in robotic disassembly of LIBs are to some extent feasible. However, the handling and removal of the separated components impose substantial challenges regarding robotic manipulation (Harper et al., 2019). In other words, simple pick-and-place manipulation is not easy for robots, as it requires consideration of motion path planning, grasp position, gripper design, and tracking of motion to avoid slippage (Meng et al., 2022). Although Choux et al. (2021) have proposed and demonstrated a task planner for the robotic disassembly of an EV LIB pack to module level, the authors summarized some challenges that remain: high processing time resulting in

financial unviability, remaining need for human assistance and low success rate due to high inaccuracy of the vision system. All things considered, the inherent challenge is to develop control algorithms and software that can make existing hardware (e.g. robotic arms) handle the wast complexity of EV LIB disassembly (Harper et al., 2019). At the present time, AI is primarily used for computer vision. Further technological advancements on intelligent pre-processing, disassembly planning and the disassembly process are required to successfully accommodate the future volume of spent LIBs.

2.5   Techno-economic analysis

A Techno-Economic Analysis (TEA) is an analytic framework that combines technical and economic factors to assess the feasibility, viability, and potential outcomes of a specific technology or project (Kuppens et al., 2015; Zimmermann et al., 2020). TEAs are commonly conducted in various industries, such as energy, manufacturing, and transportation, with the overarching objective to provide insights into the economic viability and potential benefits of implementing a particular technology or project. Nonetheless, as asserted by Giacomella (2021) and Zimmermann et al. (2020), the absence of a standardized methodology poses a challenge for conducting TEAs, leading to significant variations among studies. Consequently, comparisons between studies often become akin to "apples vs. oranges", lacking the necessary comparability required for meaningful synthesis. Often times this results in studies only being comparable for specific industrial technological fields.

In this context, Giacomella (2021) highlights the significance of economic feasibility disciplines, including cost estimation, market conditions, and profitability, as fundamental elements within a TEA. However, due to the significant variations observed in TEAs, these fundamental elements necessitates a detailed breakdown into specific parameters that are tailored to each case to ensure accurate and context-specific solutions. In terms of TEAs that focuses on EV LIB recycling, the economic feasibility is often assessed through cost and revenue considerations. Cost of disassembly is an important parameter when determining the feasibility of robotic module disassembly. In the literature, this parameter is frequently presented as cost per kWh disassembled or in terms of capital expenditures for the robotic investment (Lander et al., 2023). When it comes to recycling, cost and revenue parameters are often presented in terms of monetary values per kWh recycled or per kg of cells recycled (Lander et al., 2021; Thompson et al., 2021).

Furthermore, the specification of system boundaries holds significant importance in conducting TEA. Describing the boundaries is a fundamental step in identifying the input and output flows and uncovering potential flaws (Giacomella, 2021). Moreover, system boundaries play a crucial role in determining the scope of the analysis and facilitating transparent comparisons with other TEAs (Zimmermann et al., 2020).

Chapter 3

Method

This chapter is divided into three parts. First, an overview of the system boundaries of this thesis is presented, followed by an elaboration of the unit of analysis, research design, and sampling of battery types. Next, the methodology for assessing robotic module is outlined, including assumptions of key parameters. The final section presents the methodological steps and assumptions involved in modelling a recycling process aimed at obtaining potential recycling revenues.

3.1 Overview

Following the problem formulation stated in chapter 1.2, this thesis aims at assessing the economic viability of an automated EV LIB disassembly process from module to cell level. The general idea is that revenue gains or cost savings could be obtained by mechanically processing cells instead of modules in a recycling process. If this were to be the case, automated disassembly of the battery modules would be necessary due to the expected increase of EoL EV LIBs in the coming years. However, such a disassembly process would require a non-negligible investment that would need to be reimbursed through the potential revenue gains provided by mechanically processing cells rather than modules. Figure 3.1 provides an overview of the system boundaries of this thesis, while also contrasting the options of mechanically processing modules vs processing cells. Initial steps as transportation, discharge and disassembly to module level are out of the scope of this thesis. Final steps as hydrometallurgical processing (e.g. leaching) are also out of the scope. The main focus is on robotic module disassembly and the mechanical processing side of LIB recycling.

In order to answer the research question formulated in Section 1.2.1, the following shall be executed:

1. Model a robotic module disassembly line to estimate the costs of such a disassembly line and the potential annual throughput of EV battery modules.

2. Identify under what circumstances cost savings or revenue gains could be obtained by processing cells instead of modules.

3. Estimate the potential cost savings or revenue gains from the identified circumstances for the purpose of calculating the net present value (NPV) of the robotic module disassembly line. In other words, determine whether or not robotic module disassembly is profitable.

Spent EV   Discharging   Battery pack

Module

Mechanical processing

Robotic disassebly
from module to cell

Cell   Module components

Mechanical processing

Recovered materials

Hydrometallurgical process
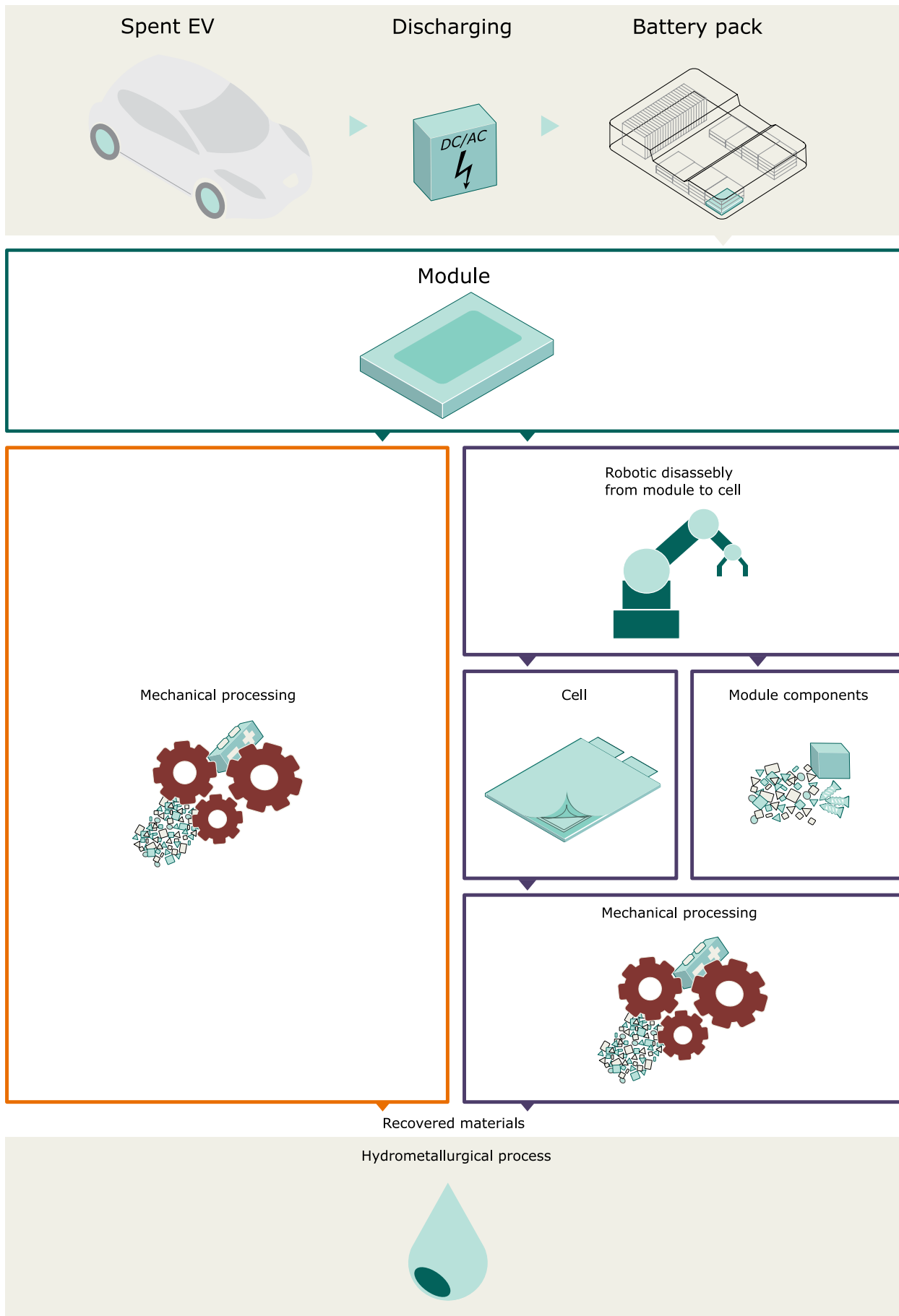
Figure 3.1: Process flowchart displaying the system boundaries.

3.1.1 Unit of analysis and research design

In this study, robotic module disassembly is evaluated by comparing the option of mechanically processing cells instead of modules. Consequently, in the first part of the analysis, the unit of analysis is the disassembly process. Subsequently, the unit of analysis during the second part of the analysis pertains to the mechanical processing steps involved in a recycling process. By disassembling the battery modules into cells and studying the disassembly- and recycling process at that level, insights can be gained into the challenges and opportunities associated with automation of disassembly, and identify ways to improve efficiency and reduce costs of the recycling process.

This study is essentially a quantitative study where the majority of data collected is numerical variables. The results of this study will to a large extent be expressed in measurable units. Consequently, a quantitative approach is essential. The numerical results should create an argumentative basis on whether or not robotic module disassembly is economic viable based on the estimated revenue gains or cost savings obtained by processing cells instead of modules. The methods used for data collection and systematic approach to analyse the data and perform the necessary calculations are covered in Sections 3.2 and 3.3. Microsoft Excel was used to perform all calculations, which are documented and presented in the Appendix. Furthermore, the Excel workbook used in this study can be accessed and downloaded from a URL link provided in Appendix A.

3.1.2 Sampling of battery types

For this study, UiA granted access for various types of battery modules from both EVs and PHEVs. To answer the research question, the authors have opted to conduct a disassembly analysis of three different battery modules to establish requirements for the robotic operations. Equally important, the battery modules included in this research differ in terms of cathode chemistry, a factor that greatly influences recycling revenue. The selected battery modules is the Volkswagen E-Golf 2019 (NMC111), the Hyundai Ioniq 2. Gen 2019 (NMC622), and the Mitsubishi Outlander PHEV 2017 (LCO). These three battery modules represents a breadth of battery architectures and chemistry's from three considerable car manufacturers, with Volkswagen E-golf reaching a shared third place for the most sold EV in Europe in 2019 (Hall et al., 2020). The Hyundai Ioniq reached a considerable 6.5% market share in the global EV market in 2019, ranking fifth in the world (Yoon, 2022). Lastly, the Mitsubishi Outlander was the number one sold PHEV in Europe in 2017, responsible for

13% of a total 150,000 PHEV units sold inside the European market (Demandt, 2018).

3.2 Methodology for assessing robotic module disassembly

To model a robotic module disassembly line, a complete teardown analysis for each of the battery modules was performed. The battery modules were manually disassembled at UiA by the authors while establishing a detailed manual disassembly process from module to cell level. A connection diagram for each module was also developed, displaying how the different components are connected. Moreover, the manual tools required for each disassembly step were considered. A complete mapping of the module components is included in the disassembly analysis, where all components are weighed and assigned a tag. This is done based on the assumption that these components (e.g. steel, aluminium, plastics) can be sold to generate revenue. It should be noted that the components of the module are those that constitute the module, with the exclusion of the battery cells. The revenue from module components was calculated using equation 3.1.

$$R_m = \sum_{z=1}^{n} \frac{M_{mz}}{Mtot_{mz}} * V_{mz} \tag{3.1}$$

Where:

R_m = Revenue from module materials [\$]

z = Index for each material from 1 to z

M_{mz} = Mass of module material z [kg]

$Mtot_{mz}$ = Total mass of module material [kg]

V_{mz} = Value of module material z [\$]

Information regarding the manual disassembly steps and the connection between components was further used to model the robotic module disassembly line. The information enabled selection of convenient robotic manipulators, required tooling and other hardware. This was done in collaboration with engineers at UiA and a well known robot supplier in Norway. Also, results from the LIBRES project (NFR: LIBRES 282328) guided the selection of robotic manipulators. Cost data was then collected on all required components for the robotic module disassembly line. This included investment costs, maintenance costs, utility costs, cost of software, installation- and shipping costs and operating lifetime. These parameters were used to calculate the total cost of the robotic module disassembly line.

Capital cost

The capital cost of an asset is given by (Bjørnenak, 2019):

$$\text{Capital cost} = \text{depreciation} + \text{cost of capital} \tag{3.2}$$

Depreciation is a systematic distribution of the investment costs during an assets economic lifetime (Bjørnenak, 2019). Cost of capital is the return forgone by investing capital in an asset rather than elsewhere (Datar & Rajan, 2018). There are several ways to calculate total capital cost, mainly depending on choice of depreciation model. For simplicity, a nominal annuity depreciation model was used. This yields a linear capital cost during the assets economic lifetime. The cost of capital involves the capital tie-up and a discount rate. The discount rate reflects the owners expected return on capital invested, often adjusted for risks (e.g. inflation). The capital cost was calculated by equation 3.3.

$$C_c = C_i * \left(\frac{r_d (1 + r_d)^n}{(1 + r_d)^n - 1} \right) \tag{3.3}$$

Where:

C_c = Capital cost [\$]

C_i = Investment cost [\$]

r_d = Discount rate [%]

n = Service lifetime [years]

Investment cost, C_i, is the sum of all hardware costs, including robots, tooling and other hardware (e.g. vision system). All other costs are included in the operating costs.

Operating costs

Operating costs includes costs of software licences, cost of electric power and cost of maintenance. Operating costs was calculated by using equation 3.4.

$$C_o = (\sum_{i=1}^{n} P_i * t_i) * P_e + C_m + C_s \tag{3.4}$$

Where:

C_o = Operating costs [$]

i = Index for each equipment from 1 to n

P_i = Power consumption of hardware i [kWh]

t_i = Working time of equipment i [h]

C_e = Cost of electricity for industrial uses [$/kWh]

C_m = Cost of maintenance of equipment [$]

C_s = Cost of required software licences [$]

The variable electricity cost for a ten-year average, as well as fixed and variable net expenses, were used to determine the cost of electricity C_e.

Annual costs

The annual costs of the robotic disassembly line is given by equation 3.5.

$$C_a = C_c + C_o \tag{3.5}$$

Where:

C_a = Annual costs

3.2.1 Robotic cycle times

As a next step, the annual throughput of EV modules in the disassembly line was estimated. This information was obtained by estimating the robot cycle time for each module (e.g. time used to disassemble each module to cell level). After establishing a detailed manual disassembly process, the robotic operations required to disassemble each module were assumed. Subsequently, the robotic cycle times were estimated. Often, the cycle time of robots are obtained using time intensive and costly simulation software. Further, this often requires comprehensive path planning and robotic data. Robotic path planning is not performed

in this thesis. Consequently, based on the required robotic operations to disassemble each module, robotic cycle times were estimated in collaboration with engineers at UiA using three-point estimation. The sum of all steps was calculated in two ways: total disassembly time and total robotic operation time. Several of the robotic operations can be performed at the same time (e.g. overlapping operations). Consequently, the total disassembly time is shorter than the total robot operation time. The total disassembly time reflects the potential annual throughput of battery modules in the disassembly line, while the total robotic operation time was used to estimate the cost of electrical power (e.g. as input to parameter t_i in equation 3.2). A methodological overview of three-point estimation follows.

Three-point estimation is a subpart of uncertainty analysis and is widely adopted in project management to calculate the expected cost and duration of project activities (Austeng et al., 2005). Several methods and approaches to three-point estimates exists. In this thesis, the Successive Principle, developed by Steen Lichtenberg was utilized (Lichtenberg Partners, n.d.). The Successive Principle is derived in detail by Drevland (2005). The input parameters consist of a three-point estimate: most likely, optimistic and pessimistic estimate. A presentation of the formulas used follows, obtained by Drevland (2005).

The expected disassembly time for each activity is obtained by equation 3.6.

$$E = \frac{o + 0.42m + p}{2.42} \tag{3.6}$$

Where:

E = Expected value

m = most likely estimate

o = Optimistic estimate

p = Pessimistic estimate

The standard deviation for each disassembly activity is obtained by equation 3.7.

$$\sigma = \frac{p - o}{2.53} \tag{3.7}$$

Where:

σ = Standard deviation

The total expected disassembly time for one module is obtained by equation 3.8, while the sum of all standard deviations is obtained by equation 3.9.

$$E_{total} = E\left(\sum X_i\right) = \sum E(X_i) \tag{3.8}$$

Where:

E_{total} = Expected duration of disassembly process

X_i = Expected activity duration

$$\sigma_{total} = \sqrt{\left(\sum_{i=1}^{n} \sigma_{Xi}^2\right)} \tag{3.9}$$

Where:

σ_{total} = Sum standard deviation of disassembly process

σ^2 = Variance

The expected value E, referring to equation 3.6 is often denoted P50 (percentile 50 in the Erlang distribution), a value there is 50% chance of reaching. To increase the certainty of the estimate, P90 can be used (90% chance of reaching the given value). Calculation of percentile 90 (P90) is expressed in equation 3.10 and was used to calculate the robot cycle times after obtaining the expected value.

$$F^{-1}(0.9) = E_{total} + \sigma_{total} * \phi^{-1}(0.9) \tag{3.10}$$

The potential annual throughput for the different battery modules was derived by equation 3.11.

$$Q = \frac{8,700}{F^{-1}(0.9)} \tag{3.11}$$

Where:

Q = Annual throughput

3.2.2 Assumptions of key parameters, robotic module disassembly

The following assumptions are made for the economic calculations regarding robotic module disassembly.

- Cost year and currency: 2023, $[1]

- Currency conversion factor for year 2023: 10.0 (NOK to $).

- Discount rate: 12%[2]

- Robotic operating hours per year: 8,700[3]

- Service lifetime is assumed equal for all equipment (6 years).

- It is assumed that the residuals value of all equipment is equal to zero.

3.2.3 Data collection, robotic module disassembly

The investment costs, maintenance costs, software costs and other costs related to the robotic cell are collected from various suppliers in Norway. The data was collected by requesting a quote on the required equipment. Cost data on supplementary hardware (e.g. vision system) was obtained from UiA.

3.3 Methodology for modelling the recycling process

This section describes the methodological steps to estimate potential revenue gains or cost savings related to recycling. Any identified revenue gains or cost savings are related to the mechanical processing steps of the LithoRec process. The LithoRec process was previously outlined in Section 2.3.3. Most recycling processes world wide is diversified with respect to process steps, materials recovered and recycling efficiency. Moreover, several recycling processes are only briefly documented for public view. Consequently, insight and data collection from such processes are difficult to obtain. On the other side, the LithoRec process is a comprehensively documented process where all required data are available. Therefore, the LithoRec process is used as a reference process in this study.

It is assumed that processing of battery cells instead of battery modules will under no circumstances increase the recycling cost related to mechanical- or hydrometallurgical processing.

---

[1]Costs are adjusted by a yearly inflation factor of 4% to the reference year 2023.
[2]Assuming 8% return on capital invested and 4% inflation.
[3]Generally, robots can work 24 hours a day, 7 days a week. However, some maintenance downtime are assumed.

Under these circumstances, the potential outcome of processing cells will be an increase or decrease in revenue per kg cell recycled. The publicly available EverBatt model ("Argonne National Laboratory," n.d.), developed by Argonne Collaborative Center for Energy Storage Science was used to obtain the revenue per kg cell recycled for the different battery chemistries. EverBatt is an Excel-based model used to analyse all stages regarding manufacturing and recycling of EV LIBs ("Argonne National Laboratory," n.d.). To clarify, the EverBatt model is based upon recycling of battery cells, not battery modules. The LithoRec process was modelled in the EverBatt model with respect to material recycling rate and recovered battery materials. The LithoRec process and the EverBatt model are based upon different hydrometallurgical recycling processes. However, as the revenue per kg cell recycled is the desired output, the LithoRec process can successfully be modelled in the EverBatt model by adjusting the recycling rate and the recovered battery materials.

The mechanical processing steps of LithoRec is modelled for two capacity classes: 1,200 tons and 6,000 tons of battery material per year. Potential revenue gains or cost savings was identified and economically evaluated in both capacity classes for the different battery chemistries based upon the NPV of future cash flows. The NPV is the sum of discounted cash flows during the planning periods. An investment is economically favourable if the NPV is positive (Kwade & Diekmann, 2017).

$$NPV = -C_i + \sum_{t=1}^{n} \frac{CF_t}{(1+i)^t} \qquad (3.12)$$

C_i reflects the initial investments into the robotic module disassembly line. CF_t is the cash flow in each period t which are composed of operation costs related to the disassembly line (C_o) and potential revenue gains or cost savings obtained by processing cells instead of modules.

3.3.1 Assumptions of key parameters, recycling process

- Cost year and currency: 2023, $

- Currency conversion factor for year 2023: 10.0 (NOK to $).

- Discount rate: 12%

- It is assumed 100% recovery rate of module components recovered in the robotic disassembly line.

- It is assumed 80% recovery rate of module components recovered in the recycling process.

- All recovered module components are sold to a third-party.

- It is assumed that the cells contain zero amount of steel.

- Processing of battery cells instead of battery modules will under no circumstances increase the recycling costs related to mechanical- or hydrometallurgical processing.

3.3.2 Data collection, recycling process

The data used regarding recycling was obtained from the LithoRec process and the EverBatt model. Table 3.1 displays the mechanical processing parameters obtained from LithoRec (Kwade & Diekmann, 2017).

Table 3.1: Mechanical processing parameters of LithoRec

Process step	Capacity	Investment [$]	Operating costs [$]
Mechanical processing	Small (1,200 t modules/a)	2,106,223	385,664
Mechanical processing	Large (6,000 t modules/a)	4,020,857	668,069

The materials recovered in the LithoRec process with their respective unit prices are summarized in Table 3.2. The unit prices were obtained from the EverBatt model ("Argonne National Laboratory," n.d.). EverBatt uses marcos to keep material unit pricing up to date with market prices. The LithoRec process reaches an overall material recycling rate of 80% for an EV battery system. Graphite is not recycled.

As earlier mentioned, when processing battery modules, the module components (aluminum, plastic, steel) are recovered by a rate of 80% in accordance with Table 3.2. On the contrary, when disassembling the battery modules and processing battery cells, the recovery rate of

Table 3.2: Unit prices of recovered battery materials

Materials	Unit prices [$/$kg$]	Recovery rate [%]
Aluminium	1.45	80%
Plastics	0.10	80%
Copper	5.43	80%
Nickel	13.00	80%
Steel	0.28	80%
Cobalt	52.00	80%
Manganese	3.00	80%

the above mentioned materials are assumed 100%. Recovering the module components prior to the recycling process produces less mixed waste streams and should create economic gain.

The cell material composition of the different battery chemistries included in this thesis is presented in table 3.3. Data obtained from the EverBatt model ("Argonne National Laboratory," n.d.).

Table 3.3: Cell material composition [wt%]

Materials	NMC111	NMC622	LCO
Cathode	38.8%	36.0%	35.3%
Graphite	20.0%	21.6%	18.5%
Carbon black	0.8%	0.7%	2.4%
Binder: PVDF	0.8%	0.7%	2.4%
Binder: anode	1.1%	0.4%	0.6%
Copper	16.8%	18.1%	16.1%
Aluminium	8.5%	9.1%	8.1%
Electrolyte: LiPF6	1.7%	1.7%	2.2%
Electrolyte: EC	4.6%	4.6%	6.0%
Electrolyte: DMC	4.6%	4.6%	6.0%
Plastic: PP	1.6%	1.7%	1.8%
Plastic: PE	0.4%	0.4%	0.3%
Plastic: PET	0.3%	0.3%	0.3%
Steel	0.0%	0.0%	0.0%

Chapter 4

Results

This chapter is divided in two parts and presents results on (1) the cost of the robotic module disassembly line in addition to the potential annual throughput of EV modules and (2) potential recycling revenues and the NPV of the robotic module disassembly line given different circumstances.

4.1 Robotic module disassembly

This section presents the costs of the robotic module disassembly line and the potential annual throughput of EV modules. First, the complete teardown analysis for each module is reviewed.

4.1.1 Module specifications

Volkswagen E-Golf 2019 NMC111

The Volkswagen E-Golf 2019 battery module, which will be referred to as "Volkswagen" henceforth, are depicted in Figure 4.1. The battery module consist of 12 individual cells. Module and cell dimensions are detailed in Table 4.1.

Table 4.1: Dimensions and weight, Volkswagen

Level	Length [mm]	Width [mm]	Height [mm]	Weight [g]	Capacity [kWh]
Module	350	150	107	10,896	1.6
Cell	145	25	90	797	0.134
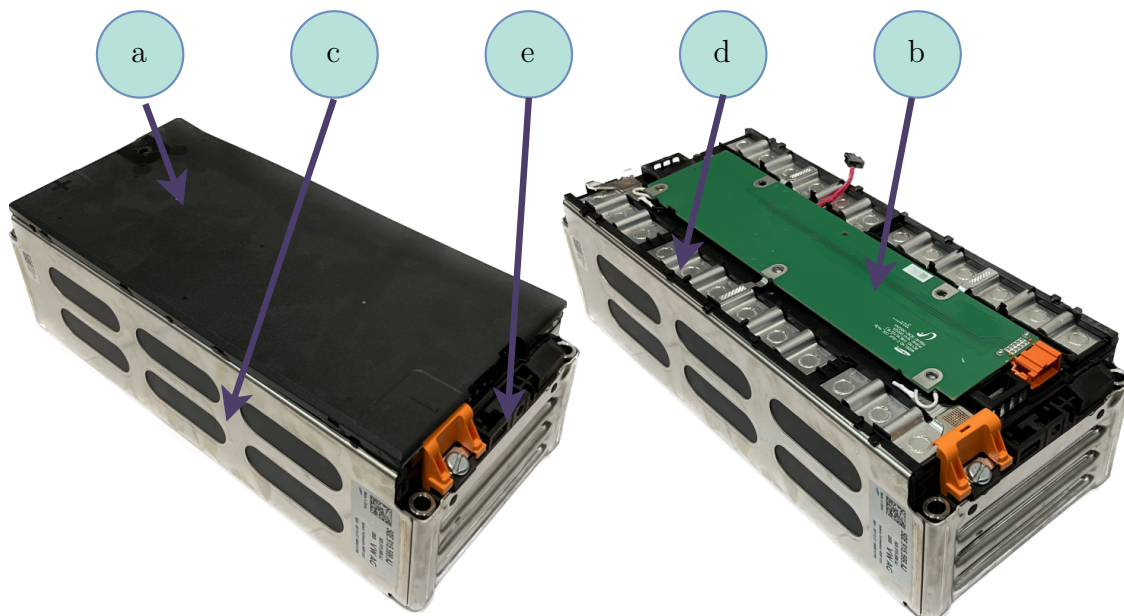
Figure 4.1: Battery module, Volkswagen

The battery module components are summarized in Table 4.2 with respect to quantity, mass and type of material. The module components mainly consist of steel, aluminium and plastics. Electronic parts can also be found, such as the cell management controller (CMC). Electronic parts are not accounted for when describing materials of the module components, given their minor weight. Note that the CMC, viewed in green in Figure 4.1, is connected to a plastic platform. The plastic platform is denoted "CMC unit" in Table 4.2. The component tags are in accordance with with Figure 4.1.

Table 4.2: Main components, Volkswagen

Component	Tag	Qty.	Mass [g]	Total mass [g]	Material
Plastic cover	a	1	100	100	Plastic
CMC unit	b	1	180	180	Plastic
Compressive plates	c	1	888	888	Steel
Cell bridge	d	8	NA	NA	Aluminium
Side module junction	e	2	82	164	Aluminium
Individual cell	f	12	797	9 564	-

A connection diagram of the Volkswagen is presented in Figure 4.2. The letters in the circles corresponds to the component tags in Table 4.2. The connection between parts are presented in tabular form in Figure 4.2. For example, the plastic cover (a) is connected to the CMC unit (b) by snap-fit and screw.

a-b	Snap-fit, screw
d-b	Laser weld
e-d	Screw and weld
d-f	Laser weld
c-f	Compression
c-e	Compression
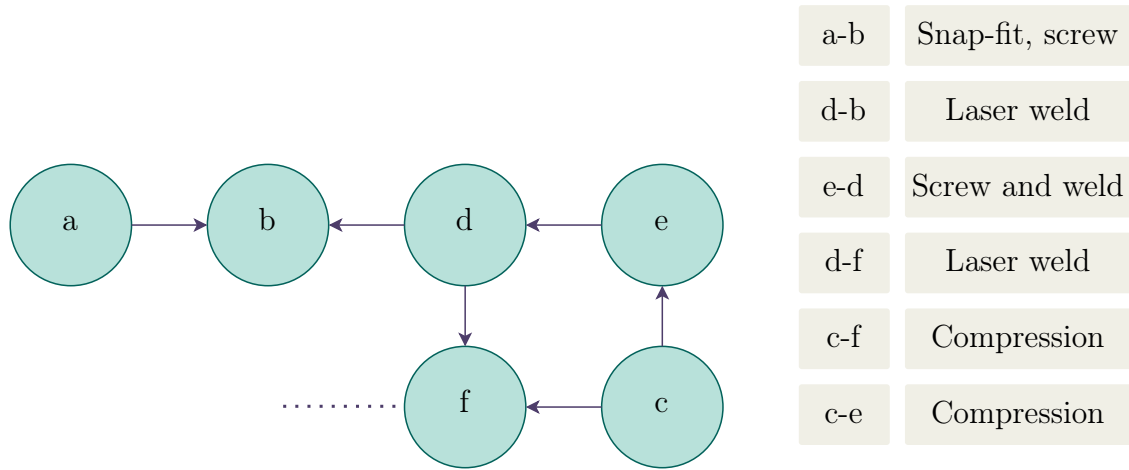
Figure 4.2: Connection Diagram, Volkswagen

Hyundai Ionic 2. Gen 2019

The Hyundai Ioniq 2. Gen 2019 battery module, which will be referred to as "Hyundai" henceforth, are visualized in Figure 4.3. The battery module consists of a total of 40 cells. Module and cell dimensions are provided in Table 4.3. The module is composed of two distinct stacks of cells that are separated by a cooling radiator (h). The two stacks, comprised of 20 cells, share the same module platform (i).

Table 4.3: Dimensions and weight, Hyundai

Level	Length [mm]	Width [mm]	Height [mm]	Weight [g]	Capacity [kWh]
Module	390	310	235	43,922	8.72
Cell	180	35	170	868	0.218
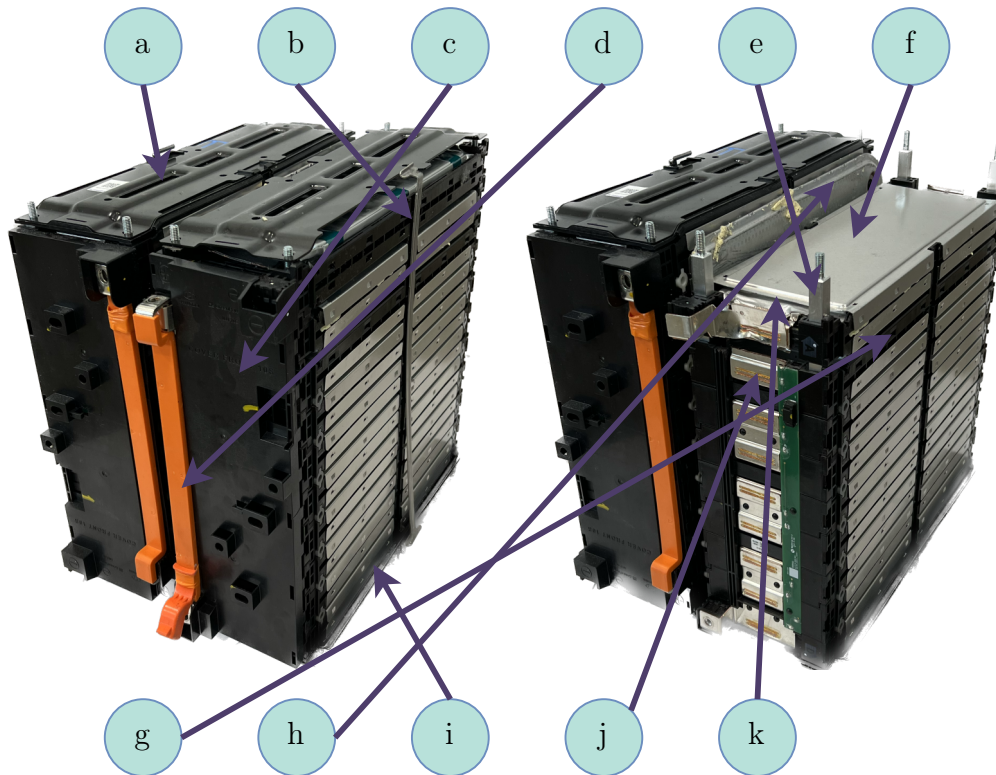
Figure 4.3: Battery module, Hyundai

The Hyundai module components are presented in Table 4.4. Note that "Other components", referring to Table 4.4, is various steel and plastic scrap.

Table 4.4: Main components, Hyundai

Component	Tag	Qty.	Mass [g]	Sum mass [g]	Material
Top cover	a	2	372/99	744/198	Steel / Plastic
Top cover brace	b	4	35	140	Aluminium
Side cover	c	4	74	296	Plastic
Side cover brace	d	2	114	228	Steel
Module brace	e	8	88	704	Steel
Cell cover	f	40	40	1 600	Aluminum
Cell frame	g	20	140	2,800	Plastic
Cooling radiator	h	1	824	824	Aluminium
Module platform	i	1	1 829/198	829/198	Steel / Plastic
Cell bridge	j	4	NA	NA	Steel
Individual cell	k	40	868	34,720	-
Other components	-	-	248/423	248/423	Steel / Plastic

The Hyundai's module connection diagram is displayed in Figure 4.4. The letters in the circles corresponds to the component tags in Table 4.4. The connection between parts are presented in tabular form in Figure 4.4. For example, cell frame (g) is connected to the cell bridge (j) with laser welded steel plates.

d-c	Screws
c-g	Snap-fit
f-g	Snap-fit
g-j	Laser weld
g-e	Compression
j-k	Laser weld
e-i	Integrated
e-a	Integrated
b-i	Snap-fit
b-a	Snap-fit
g-h	Compression Screws
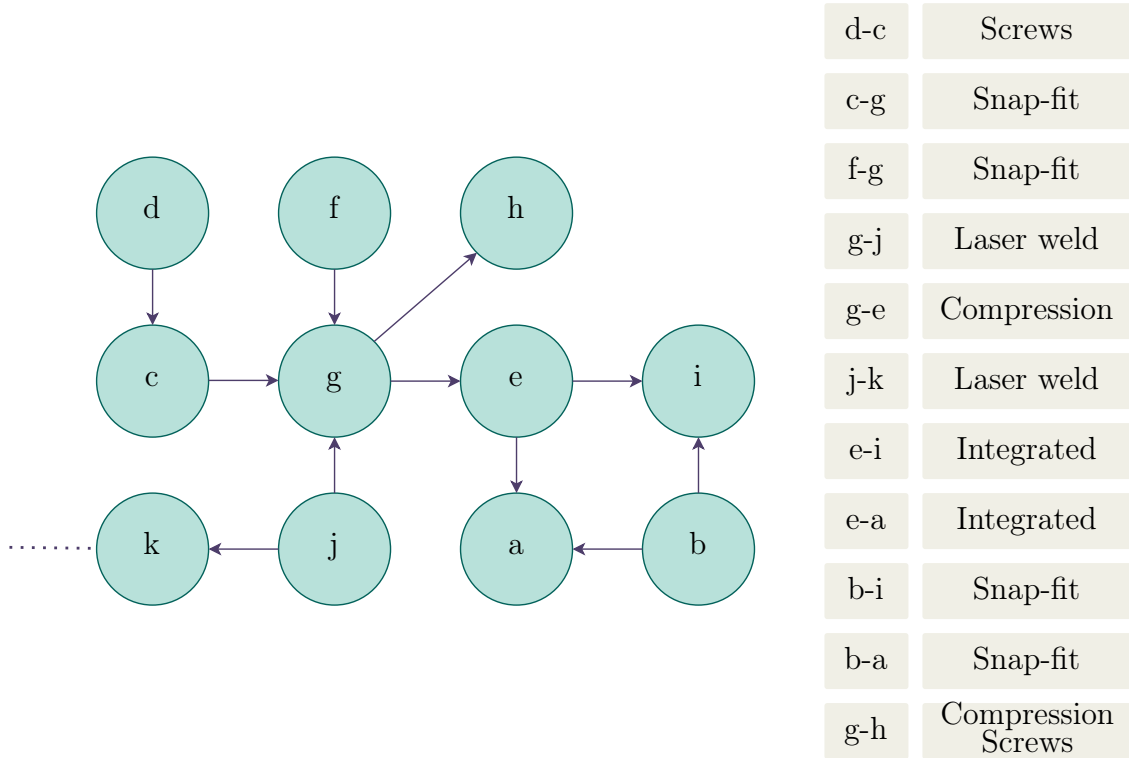
Figure 4.4: Connection Diagram, Hyundai

Mitsubishi Outlander PHEV 2017

The Mitsubishi Outlander PHEV 2017 battery module, which will be referred to as "Mitsubishi" henceforth, is shown in Figure 4.5. Similar to the Hyundai, this battery module consists of two smaller modules enclosed by the same top and bottom cover. The two enclosed modules are treated as a single module in this study and contains a total of 16 cells. The dimensions of the module and cells are detailed in Table 4.5.

Table 4.5: Dimensions and weight, Mitsubishi

Level	Length [mm]	Width [mm]	Height [mm]	Weight [g]	Capacity [kWh]
Module	625	185	130	25,478	2.28
Cell	180	35	170	1,396	0.134
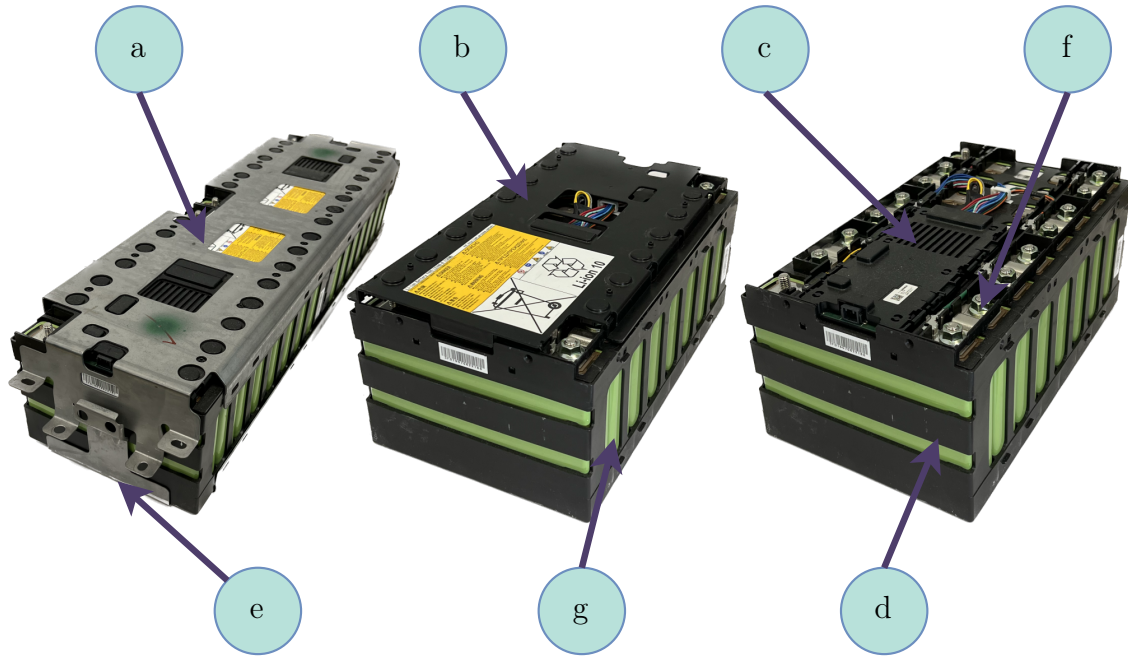
Figure 4.5: Battery module, Mitsubishi

The components of the Mitsubishi module are presented in Table 4.6. Similar to the Volkswagen, this CMC is connected to a plastic platform. The CMC and the plastic platform are joined together and referred to as the "CMC unit" in Table 4.6.

Table 4.6: Main components, Mitsubishi

Component	Tag	Qty.	Mass [g]	Sum mass [g]	Material
Top metal cover	a	1	1,108	1,108	Steel
Top plastic cover	b	2	98	196	Plastic
CMC unit	c	2	214	428	Plastic
Cell frame	d	2	241	482	Plastic
Bottom metal cover	e	1	733	733	Steel
Cell bridge	f	28	7	195	Steel
Individual cell	g	16	1 396	22,336	-

Figure 4.6 depicts the connection diagram of the Mitsubishi module. The letters in the circles corresponds to the component tags in Table 4.6. The interconnections among the components are presented in tabular form in the same figure. For instance, the top metal cover (a) is secured to the cell frame (d) by means of snap-fits.

a-d	Snap-fit
e-d	Snap-fit
d-c	Snap-fit
b-c	Snap-fit
f-c	Screw
d-g	Compression
c-g	Contacts
f-g	Screw
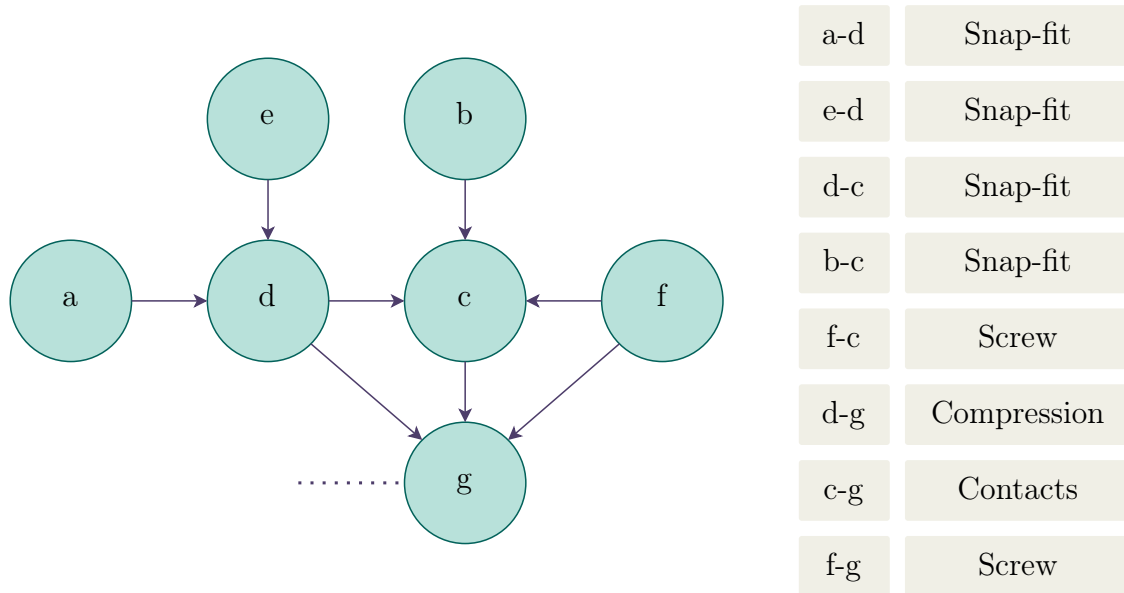
Figure 4.6: Connection Diagram, Mitsubishi

4.1.2 Module components

Table 4.7 summarizes the amount of module components recovered from the different modules in accordance with Tables 4.2, 4.4 and 4.6. The percentage per weight was calculated based on the total weight of each module, referring to Tables 4.1 4.3, and 4.5. The information in Table 4.7 is used later in this study to calculate potential revenues from module materials.

Table 4.7: Amount of module materials

	Volkswagen (Wt%)	**Hyundai** (Wt%)	**Mitsubishi** (Wt%)
Aluminum [g]	164 (1.5%)	2,564 (5.8%)	0 (0.0%)
Plastic [g]	280 (2.6%	3,915 (8.9%)	1,106 (4.3%)
Steel [g]	888 (8.1%)	2,753 (6.3%)	2,036 (8.0%)

4.1.3 Manual disassembly

Section 4.1.1 presented the different module components and the various connections between parts. This information was obtained after manually disassembling the battery modules. This section presents the manual disassembly operations performed on the different modules by the authors. The manual disassembly was carried out at UiA using a grinder and different screwdrivers. All welds and wires were cut using the grinder. All snap-fit covers were detached with a flat screwdriver, and all screws were unscrewed with an umbraco and a flat screwdriver. Note that the disassembly steps described in Tables 4.9 and 4.10 does not include disassembly of all connected parts in the connection diagrams previously presented for the Hyundai and the Mitsubishi, given that removal of the cells are achieved without disassembling all module components.

Disassembly Volkswagen

The manual disassembly steps and required tooling for the Volkswagen battery module are summarized in Table 4.8. The letters in parenthesis, referring to Table 4.8, corresponds to the component tags in Table 4.2.

Table 4.8: Manual disassembly steps, Volkswagen

Step	Description	Required tool
I	Removal of plastic cover (a)	Screwdriver
II	Removal of compressive plate (c)	Grinder
III	Cut bridge between each cell connector (d)	Grinder
IV	Removal of CMC unit (b) with connector	Screwdriver and grinder
V	Separate side module junction (e)	Screwdriver and hand

Disassembly Hyundai

The disassembly steps and required tooling for the Hyundai battery module are presented in Table 4.9, with component tags corresponding with Table 4.4.

Table 4.9: Manual disassembly steps, Hyundai

Step	Description	Required tool
I	Removal of top cover (a)	Screwdriver
II	Removal of side cover brace (d)	Screwdriver
III	Removal of side cover (c)	Screwdriver
IV	Disconnect cell frame (g) from cooling radiator (h)	Screwdriver
V	Disconnect cell frame (g) from cell bridge (j)	Grinder
VI	Removal of cell cover (f)	Screwdriver
VII	Disconnect individual cell (k) from cell bridge (j)	Grinder
VIII	Removal of 2 cells (k)	Hand
IX	Removal of cell frame (g)	Hand
X	Repeat steps VI-IX until complete disassembly	-

Disassembly Mitsubishi

The disassembly steps and required tooling for the Mitsubishi battery module are presented in Table 4.10, with component tags corresponding with Table 4.6.

Table 4.10: Manual disassembly steps, Mitsubishi

Step	Description	Required tool
I	Removal of top metal cover (a)	Screwdriver
II	Removal of bottom metal cover (e)	Screwdriver
III	Removal of top plastic cover (b)	Screwdriver
IV	Removal of CMC unit (c)	Screwdriver

4.1.4 Modelling the robotic module disassembly line

This section presents the hardware required for the robotic module disassembly line based on the required disassembly operations. The aim of this study is not related to the technical aspects of robotic manipulation, but rather to assess the economic implications of it. However, the technological steps in the automated disassembly process must be modelled to facilitate the assessment.

Following the information obtained in Section 4.1.3, the manual disassembly operations required for the different battery modules are divided into three main steps: cutting, unscrewing and removal of snap-fit covers. It is important to realize the large number of snap-fit

connections on the different battery modules. For example, each of the four side covers on the Hyundai module is connected by a total of 24 snap-fits. Additionally, the bottom and top metal covers on the Mitsubishi are connected by a total of 32 snap-fits. Robotic disassembly of snap-fit covers are discussed by Schumacher and Jouaneh (2013) who successfully demonstrates a prototype system detaching and removing snap-fit covers on remote controls and calculators. However, it is currently an inefficient process not capable of module disassembly at an industrial scale. Therefore, the next section considers existing disassembly techniques, with regards to requirements for a robotic disassembly process at an industrial scale.

Selection of disassembly technique

Generally speaking, disassembly techniques can be divided into three methods: non-destructive, semi-destructive and destructive disassembly (Umeda et al., 2015). Disassembling a product in the reverse order of assembly sequence are often labelled non-destructive disassembly, where all components and fasteners are removed individually without any injury (Umeda et al., 2015). A non-destructive approach is convenient for maintenance or when all components are designated for reuse (Nguyen, 2019). Likewise, removal of reversible fasteners could be performed with a non-destructive approach. Semi-destructive disassembly builds on the idea that components designated to be recycled or discarded can be broken in order to increase the efficiency of the disassembly process, while the components that are designated to be reused are disassembled without any injury (Umeda et al., 2015). This approach could involve destroying or damaging fasteners and other connections (e.g. drill screw heads) while inflicting minimal damage on main components (Nguyen, 2019). Lastly, destructive disassembly involves complete dismantling of a product by breaking down all components. This approach is often applied when all components are designated for recycling.

A non-destructive approach would result in high robotic cycle times, decreasing the economic viability of the overall recycling process. Also, such an approach could be problematic with regards to uncertain product conditions (e.g. irreversible screws and corrosion). In theory, a fully destructive disassembly process could be performed given that all module components and cells are designated for recycling. However, damaging the cells during disassembly could impose safety hazards. Therefore, to increase the economic feasibility of the robotic disassembly line in question, a semi-destructive disassembly approach is identified as the most convenient. Conclusively, applying for a higher degree of destructive disassembly, the manual disassembly operations described in 4.1.3 will be drastically simplified.

All snap-fits connections on top, bottom and side covers are to be broken by a milling tool. The milling tool is also used to destroy all welds and bridges between cell connectors. Dismantling of screws could also be carried out by milling all screw heads, particularly when the screws are irreversible. Although this may be true, milling of all screw heads could inflict severe wear and tear on the milling tool, increasing the operating costs. In theory, computer vision algorithms could be made to distinguish between reversible and corroded irreversible screws. Consequently, reversible screws could be unscrewed, while irreversible screws could be dismantled by milling the screw head. However, since solutions for computer vision algorithms is out of the scope of this thesis, all screws are assumed unscrewed by a robot equipped with a screwdriver.

Selection of hardware

Significant time could be lost on tool change in a robotic disassembly line (Nguyen, 2019). To minimize this loss of time, it was concluded that the robotic disassembly line should consist of three robots with required tools. This includes one robot with a milling tool, a second robot with a spindle tool (e.g. screwdriver) and a third robot with a gripper tool. Tool change is only required when unscrewing screws of different dimensions and gripping various objects (changing between a vacuum gripper and a finger gripper).

When using three different robots with varying tools, a stationary workstation is most convenient. This allows the robots to work in parallel, increasing the disassembly efficiency. The workstation consist of a rotary worktable and a fixture system for the battery module. Moreover, a conveyor belt is utilized for the transportation of battery modules to and from the workstation. Finally, a vision system is installed for component detection purposes. The required hardware is summarized in Table 4.11.

Table 4.11: Required hardware for disassembly line

Hardware nr.	Description	Function
1	Rotary worktable	Workstation
2	Fixture system	Workstation
3	Vision system	Workstation
4	Machine guarding	Workstation
5	Conveyor belt system	Transportation
6	Robot with milling tool	Robot cell
7	Robot with spindle	Robot cell
8	Robot with vacuum and finger gripper	Robot cell
9	Tool station	Robot cell

A presentation of the selected hardware based on the above mentioned requirements follows:

ABB IRB 6660

The ABB IRB 6660 is a stiff and robust industrial robot designed for press tending, machining, cutting and milling. To increase dependability and uptime, the robot has a dedicated protection kit for vital parts and cables. Additionally, the robot is equipped with integrated force control. The IRB 6660 will be equipped with a milling tool, carrying out all cutting operations.

ABB GoFa CRB 15000

The ABB GoFa CRB 1500 is a collaborative robot mainly designed for pick and place operations. However, due to its limited payload capacity of 5 kg, the robot will be equipped with an OnRobot Screwdriver, carrying out all required unscrewing operations.

ABB Swifty CRB 1300

The ABB Swifty CRB 1300 is a collaborative robot mainly designed for assembly operations. With a greater load capacity than the GoFa, the Swifty will be equipped with an OnRobot Finger Gripper (VG6) and an OnRobot Vaccum Gripper (VGP20) to carry out all pick and place operations.

The three robot are delivered with integrated force control. The Swifty requires a Flange Adapter Kit to mount the grippers to the robot. Also, a Quick Changer Kit enables efficient swapping between the finger gripper and vacuum gripper. The IRB 6660 and GoFa are supported without the use of a flange adapter. Regarding power consumption, the IRB 6660 is rated at 1.6 kW at max load during an ISO Cube 1000 m/s movement. However, in this application, the IRB 6660 will not be used at max load. Therefore, an average power consumption of 1.0 kWh is assumed. Data on power consumption related to GoFa and Swifty was not obtained. In comparison, a smaller robot delivered by Universal Robots (UR10), is rated at 0.350kWh on average. Consequently, an average power consumption of 0.5 kWh is assumed for both the GoFa and Swifty. Specifications for the three robots are summarized in Table 4.12.

Table 4.12: Robot specifications

Robot	Load capacity [kg]	Reach [m]	Weight [kg]	Power consumption [kWh]
ABB IRB 6660	130	3.10	1,910	1.00
ABB GoFa	5	0.95	28	0.50
ABB Swifty	11	0.90	75	0.50

IRBP A Workpiece Positioner

The ABB IRBP A Workpiece Positioner functions as a rotary worktable, used for manipulating workpieces in arc welding, cutting and other applications. It allows the workpiece to be rotated around two axes with a maximum payload of 250 kg. The workpiece positioner is used to manipulate the battery modules. The power consumption is negligible and therefore excluded from the economic calculations.

Fixture system

The fixture system is used to centre the modules on the workpiece positioner while robotic operations are performed. The fixture system is composed of four pneumatic cylinders clamping the modules in place. The system is developed by the engineers at UiA. The power consumption is negligible, and therefore not included in the economic calculations.

Vision system

The Zivid One+ is a 3D vision camera specifically designed for use in industrial and collaborative robotic cells. Its primary applications include robotic pick and place operations, inspection, and manufacturing. By establishing a network that interconnects all robots, the vision system enables the robots to work simultaneously on a module. The camera is installed above the worktable, serving as a source for component detection and navigation capabilities.

Conveyor belt

A conveyor belt system is used to transport the modules to the rotary worktable and manage the handling of recovered cells that result from the disassembly process. The system comprises two automated conveyor belts, each measuring 7.5 meters in length.

Machine guarding equipment

A machine guard is used to limit or prevent access to areas that are deemed hazardous. Specifically, the machine guard is installed to enclose the disassembly line where the robots are operating.

Tool station

A tool change station is required for ABB GoFa CRB 15000 to change between various bits. This is developed by engineers at UiA. These costs are not accounted for.

Cost of hardware and operation

Table 4.13 displays the collected data on hardware and operating costs.

Table 4.13: Cost parameters for the automated disassembly line

Hardware costs	Cost [$]	Operating costs	Cost [$]
ABB IRB 6660	125,000	RobotStudio Lisence	4,000
ABB GoFa	41,500	Ploy Software Lisence	4,568
ABB Swifty	40,076	Maintenance cost [a]	4,000
OnRobot Screwdriver	25,652	Electricity costs [b]	1,000 - 2,000
OnRobot Finger Gripper	11,484	**Sum** (C_o)	≈ 14,000
OnRobot Vacuum Gripper	11,651		
IRBP A	19,000		
Conveyor belt	7,800		
Machine guarding	2,411		
Zivid One+	19,200		
Fixture system	10,000		
Setup and shipment	6,422		
Sum (C_i)	325,197		

[a]Annual maintenance cost for the robots is rated at 800$ in accordance with the data collected from the robot supplier. Maintenance cost for the IRBP A and Conveyor belt was not obtained. Therefore, the same maintenance cost as the robots are assumed. Maintenance cost for the vision and fixture system are negligible and not included.
[b]Electricity costs depends on the type of module being disassembled due to distinctive robotic operating time. Calculation of electricity costs are outlined in Appendix C.

For simplicity, an assumption is made that all hardware has equal service lifetime. The expected service lifetime for the three robots is, according to the manufacturer, 50,000 operating hours. However, the expected service lifetime for the OnRobot Screwdriver, Finger Gripper and Vacuum gripper is rated at 25,000 operating hours. Therefore, the tooling investment costs, which are specified in Table 4.13, includes the expenses for two OnRobot Screwdrivers, two Finger Grippers, and two Vacuum Grippers, achieving equal expected service lifetime as the robots. Service lifetime for the remaining hardware was not obtained and is therefore rated at 50,000 hours. For simplicity, the service life of all equipment is assumed to be 6 years.

4.1.5 Robotic disassembly

This section describes the theoretical robotic operations performed on the battery modules. The main steps are described in Tables 4.14, 4.15 and 4.16, respectively. Also, the type of robot required for the specific operation is stated in each step. A more comprehensive overview of the required robotic steps is found in appendix B, which includes operations such as movement between objects, screw removal, tool changes, and gripping operations of differently sized objects.

Robotic disassembly, Volkswagen

Table 4.14: Robotic disassembly steps, Volkswagen

Step	Description	Required robot(s)
I	Removal of plastic cover (a)	GoFa, Swifty, IRB 6660
II	Removal of compressive plate (c)	Swifty, IRB 6660
III	Cut bridge between each cell connector (d)	IRB 6660
IV	Separate side module junction (e)	GoFa, Swifty
V	Removal of CMC unit (b) with connector	Swifty
VI	Flip positioner	IRBP A

Robotic disassembly, Hyundai

Table 4.15: Robotic disassembly steps, Hyundai

Step	Description	Required robot(s)
I	Removal of top cover (a)	Swifty, IRB 6660
II	Disconnect cell frames (g) from cooling radiator (d)	GoFa
III	Cut side cover (c), cell bridge (j) and side of cell frame (g)	IRB 6660
IV	Remove cell cover (f)	Swifty, IRB 6660
V	Removal of 2 cells (k)	Swifty
VI	Removal of 2 cell frames (g)	Swifty
VII	Repeat steps IV-V until complete disassembly	-

Robotic disassembly, Mitsubishi

Table 4.16: Robotic disassembly steps, Mitsubishi

Step	Description	Required robot(s)
I	Removal of top metal cover (a)	Swifty, IRB 6660
III	Removal of top plastic cover (b)	Swifty, IRB 6660
IV	Removal of CMC unit (c)	GoFa, Swifty, IRB 6660
V[a]	Removal of 1 cell (g)	Swifty
VI	Flip positioner	IRBP A

[a]The cells are compressed in the cell frame (d). Removal of 1 cell releases the pressure. Consequently, remaining cells are removed when the rotary worktable is flipped.

4.1.6 Robotic cycle times

The total operation- and disassembly time for each module are presented in Table 4.17, together with the potential annual throughput for each module, calculated in accordance with equation 3.11. Again, the operation time is used as input to calculate the annual cost of electric power for each robot, which is outlined in Appendix C. The three-point estimates for each individual robotic operation, which are calculated by using Equations 3.6 through 3.11, are available in Appendix B.

Table 4.17: Potential annual throughput

	Volkswagen	Hyundai	Mitsubishi
Operation time [sec] (t_i)	142	803	300
Disassembly time [sec] ($F^{-}1(90)$)	77	594	254
Throughput [nr. of modules] (Q)	405,878	52,686	123,110
Throughput [nr. of cells]	4,870,536	2,107,440	1,969,760
Throughput modules [ton]	4,422	2,314	3,137
Throughput cells [ton]	3,882	1,829	2,750

For the Volkswagen, 405,878 disassembled modules correlates to a total weight of 4,442 tons of modules and 3,882 tons of cells. The disassembled module components yield 40.59 tons of aluminum, 113.65 tons of plastic and 360.42 tons of steel. For the Hyundai, 52,686 disassembled modules equals a total weight of 2,314 tons of modules and 1,820 tons of cells. Disassembled module components yields 135.09 tons of aluminium, 206.27 tons of plastic and 145.04 tons of steel. Likewise, disassembly of the Mitsubishi provides 3,137 tons of modules and 2,750 tons of cells, yielding 0 tons of aluminum, 136.16 tons of plastic and 250.65 tons of steel.

Figure 4.7 displays the cumulative distribution function of the probability distribution of disassembly time for the different modules. For Volkswagen, the probability that disassembly time is less than or equal to 77 seconds is 90%. Similarly, for Hyundai and Mitsubishi, the disassembly time at 90% probability is 594 seconds and 254 seconds, respectively.
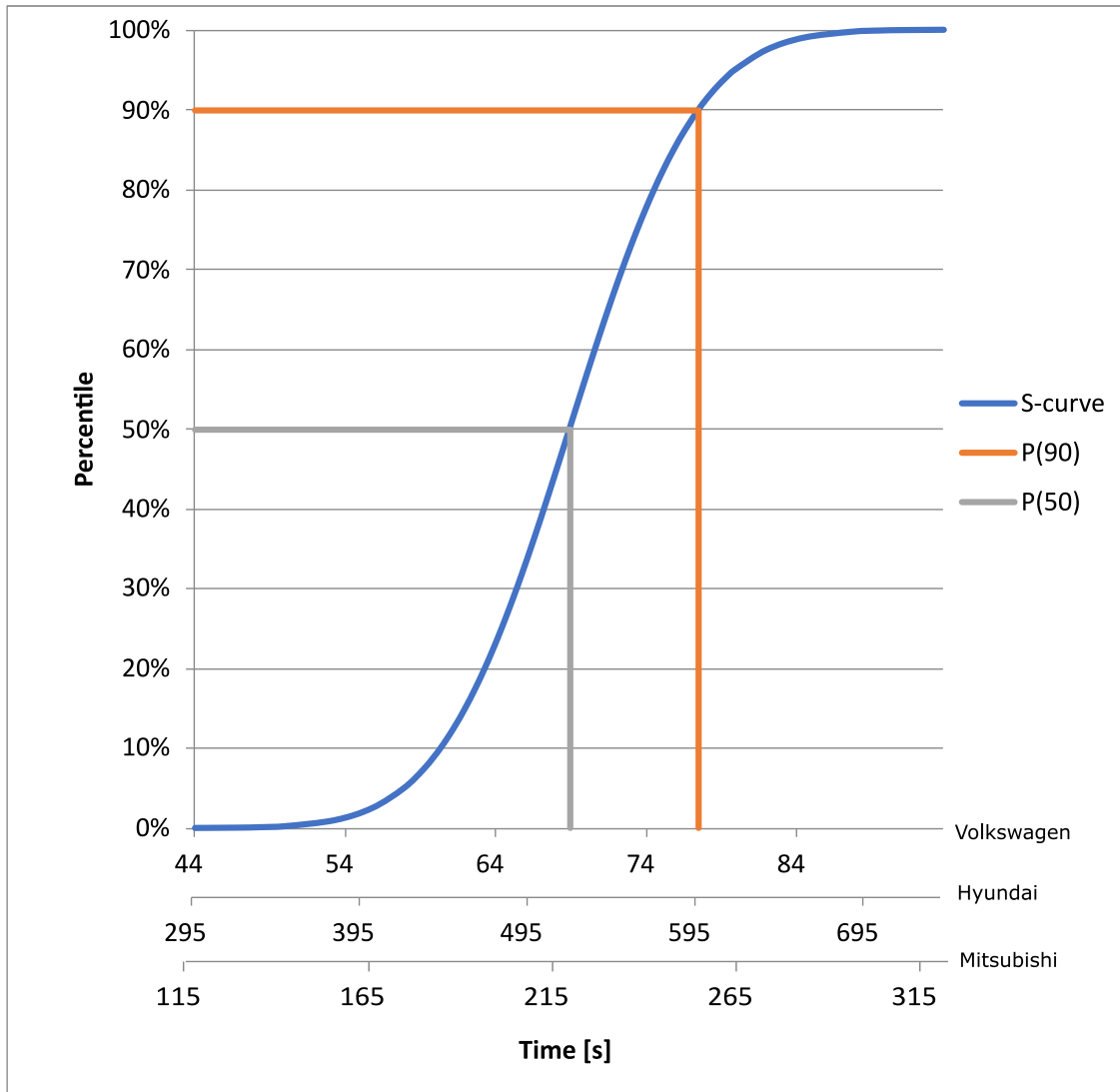
Figure 4.7: Cumulative distribution function, disassembly times

4.1.7 Annual cost for automated disassembly

Cost and cycle data were presented in the previous sections. Using Equation 3.3, the capital cost of all equipment was calculated. Further, annual operating costs were calculated by Equation 3.4, where the cost of electric power is outlined in Appendix C. Annual costs were estimated by Equation 3.5. Table 4.18 presents the results.

Table 4.18: Annual cost for automated disassembly

Module	Capital cost (C_c)	Operating cost (C_o)	Annual cost (C_a)
Volkswagen	74,405	14,688	89,093
Hyundai	74,405	14,427	88,832
Mitsubishi	74,405	14,324	88,729

Given the data on the yearly expense incurred by robotic disassembly as well as the annual throughput of modules, as presented in 4.17, it was possible to calculate the cost per

disassembled module. Furthermore, Tables 4.1, 4.3 and 4.5 provided the module capacities required for computing the cost per kWh disassembled. Results are presented in Table 4.19.

Table 4.19: Cost per module and per kWh disassembled

	Volkswagen	Hyundai	Mitsubishi
Cost per module	0.22	1.69	0.721
Cost per kWh	0.137	0.193	0.316

4.2   Recycling process

The LithoRec process was modelled in the EverBatt model for the purpose of obtaining the potential revenue per kilo cell recycled for the different battery modules. The results are presented in Table 4.20. The potential revenues vary mainly due to differences in cathode chemistry. Furthermore, the potential revenue per kilo of module components disassembled was calculated by Equation 3.1, using the data from Tables 3.2 and 4.7 as input parameters.

Table 4.20: Potential revenue per kg

Module	Potential revenue [$/kg cell]	Potential revenue [$/kg module components]
Volkswagen	5.38	0.386
Hyundai	4.39	0.529
Mitsubishi	10.15	0.217

To enable a meaningful assessment of the economic implications of automated disassembly, three scenarios that impact recycling revenue have been formulated: (1) improved capacity utilization, (2) cost reduction potential under current supply volumes, and (3) reduction of processing steps in recycling. All calculations have been carried out using Microsoft Excel. A comprehensive overview of the calculations can be found in Appendix D. It is important to note that, for Appendix D.2, D.2.1, and D.3, the input parameters used are specific to scenario 1b in Section 4.2.1. The other scenarios have been computed using the same excel workbook with varying input parameters, which is not included in the Appendix.

4.2.1   Improved capacity utilization

Processing of battery cells instead of modules could increase the volume of valuable materials going into the recycling process. The above statement is based on the assumption that any given recycler can procure an increased number of battery modules (e.g. more than the given mechanical processing capacity). The most valuable cell constituent is the cathode, consisting of valuable materials such as cobalt, nickel and manganese. The recovery of these

materials control, to some extent, the economic viability of recycling (Chen et al., 2019). When processing modules, a smaller portion of these valuable materials is subjected to the recycling process due to the less valuable module components also being mechanically processed. If pure cells were to be processed, more valuable materials could be processed due to the absence of module components. Based on these factors, potential revenue gains for the small and large capacity mechanical processing steps of the LithoRec process are presented in scenarios 1a and 1b below.

Scenario 1a

The small capacity mechanical processing step of LithoRec has a design capacity at 1,200 tons of material per year. The Volkswagen has a cell to module weight ratio of (12 cells x 0.797 kg cell) / 10.896 kg module = 0.878 in accordance with Tables 4.1 and 4.2. By processing modules in the small capacity process, a total of 1,200 x 0.878 = 1,053.6 tons of cells are recycled, in addition to 146.4 tons of module components. The potential annual revenue from recycling 1,053.6 tons of Volkswagen battery cells amounts to $5,666,775 given a revenue of $5.38 per kilo cell recycled. In addition, the module components generate a revenue of $45,325 given the potential revenue per kg module components presented in Table 4.20, and the LithoRec recycling rate of 80% (($0.387 x 146.4 x 1,000 x 0.80) = $45,325). Total recycling revenue amounts to $5,712,100.

On the other side, processing of battery cells would increase the amount of valuable materials subjected to the recycling process. In this scenario, the cells would constitute the full recycling capacity of 1,200 tons, increasing the amount of cells recycled by 146.4 tons. Under these circumstances, this would generate a revenue of $6,456,000 from the recovered cell materials. The amount of module components from 1,200 ton cells equals (1,200 - 1,053.6) / 0.878 = 167 tons, which generate a revenue of $64,547. It must be remembered that the module components are now recovered in the robotic disassembly line prior to the recycling process, yielding a 100% recovery rate following the assumptions made in Section 3.3.1. Total recycling revenue is $6,512,656. The potential annual recycling revenue gain from processing cells instead of modules is $808,447. By using Equation 3.12, the NPV for acquiring the robotic disassembly line is estimated to $2,938,268. The same scenario are modelled for the Hyundai and the Mitsubishi. The results are summarized in Table 4.21. A comparison between processing modules and cells is illustrated in Figure 4.8.
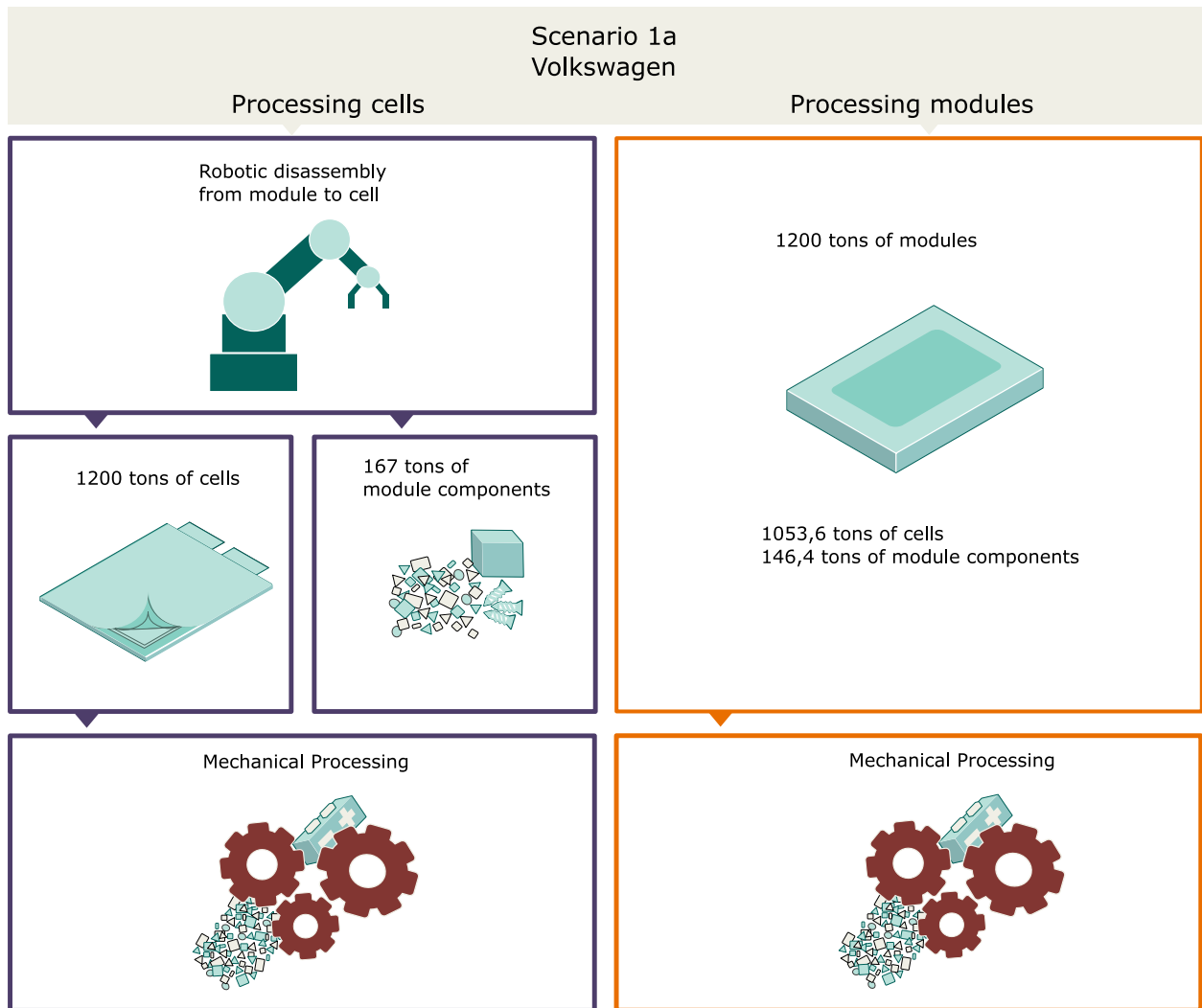
Figure 4.8: Illustration of scenario 1a.

Table 4.21: Parameters, scenario 1a

	Volkswagen	Hyundai	Mitsubishi
Cell/module weight ratio	0.878	0.790	0.877
Revenue, processing modules	$5,712,100	$4,270,318	$10,703,858
Additional cells	146.4 [ton]	252 [ton]	147.6 [ton]
Revenue, processing cells	$6,520,547	$5,436,120	$12,216,569
Annual revenue gain	$808,447	$1,165,489	$1,512,985
NPV	$2,938,268	$4,407,288	$5,836,408

Scenario 1b

The large capacity mechanical processing step of LithoRec has a design capacity of 6,000 tons of material per year. As previously mentioned, the robotic disassembly line disassembles 4,422 tons of Volkswagen battery modules which corresponds to 3,882 tons of cells. In this scenario, due to the restrained capacity of the robotic disassembly line, both modules and cells would be subjected to mechanical processing: 3,882 tons of cells from the robotic

disassembly line in addition to 6,000 - 3,882 = 2,118 tons of modules. The 2,118 tons of modules contains 2,118 x 0,878 = 1,859 tons of cells. The total amount of cells being recycled amounts to 3,882 + 1,859 = 5741 tons of cells. In comparison, by processing modules only, the total amount of cells being recycled amounts to 6,000 x 0.878 = 5,268. In this scenario, processing both modules and cells instead of modules alone increases the amount of cells recycled by 475 tons. This scenario is illustrated in Figure 4.9.

Scenario 1b
Volkswagen
Processing cells and modules | Processing modules

Robotic disassembly
From module to cell

2118 tons of modules

6000 tons of modules

3882 tons of cells | 540 tons of module components

1859 tons of cells
259 tons of module components

5268 tons of cells
732 tons of module components

Mechanical processing | Mechanical processing
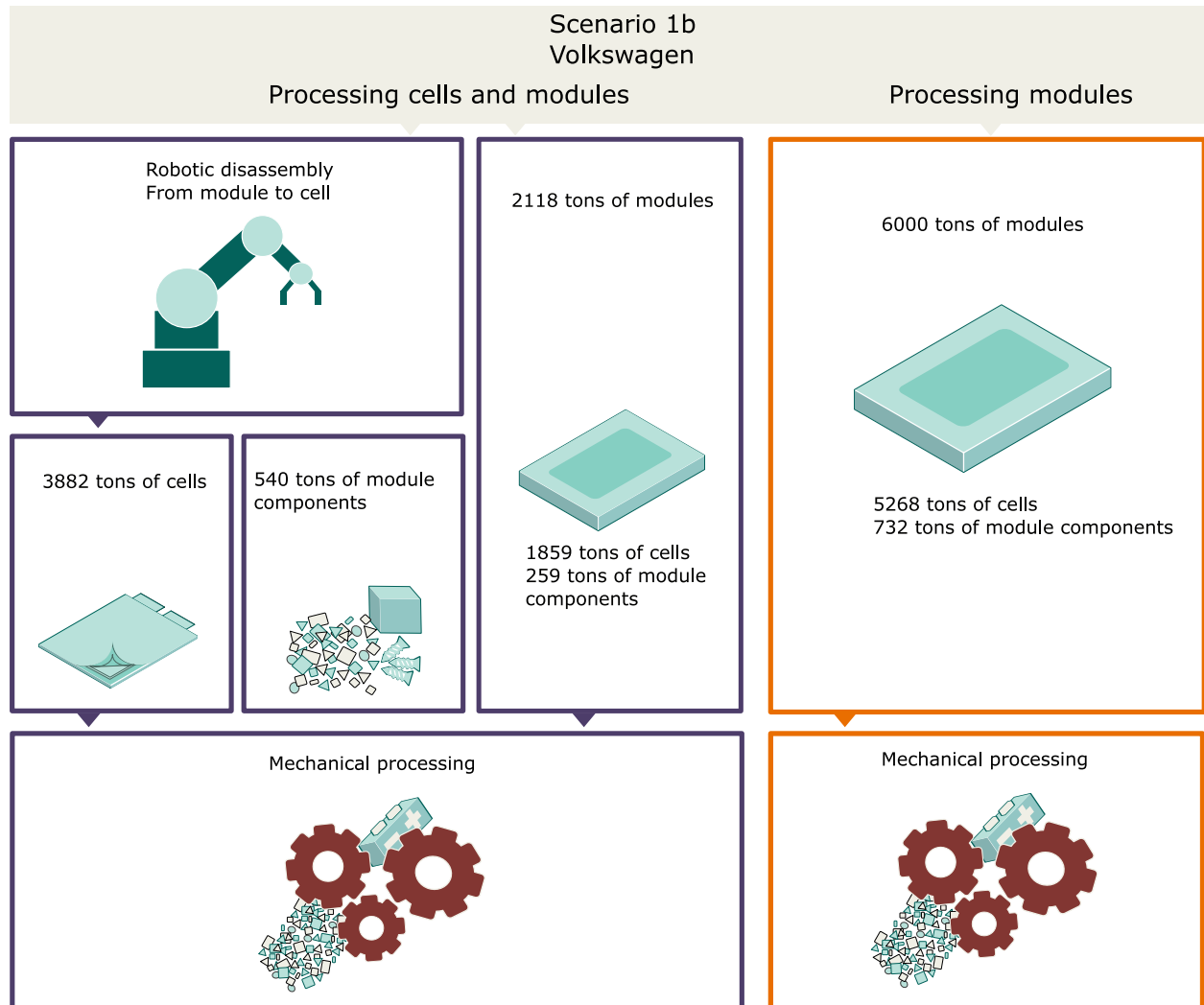
Figure 4.9: Illustration of scenario 1b.

Potential revenue gains and the NPV of the different battery modules for the above mentioned scenario are summarized in Table 4.22. Referring to the assumptions made in Section 3.3.1, the module components retained from the robotic disassembly line are recovered at 100% recovery rate, while the module components recovered from the 2,188 tons of modules in the mechanical process are recovered at 80% recovery rate.

Table 4.22: Parameters, scenario 1b

	Volkswagen	Hyundai	Mitsubishi
Revenue, shredding modules	$28,560,502	$21,353,157	$53,517,924
Additional cells	475[ton]	383[ton]	339[ton]
Revenue, shredding cells/modules	$31,199,719	$23,130,725	$56,982,991
Annual revenue gain	$2,639,217	$1,777,568	$3,465,067
NPV	$10,465,312	$6,923,792	$13,862,214

4.2.2 Cost reduction potential under current supply volumes

The recycling industry is preparing for the future challenges when large volumes of EOL EV LIBs are available to be recycled. This implies an increasing demand for larger-scale processing equipment. At the same time, the present amount of recyclable spent LIBs is limited (Statista, 2023). Consequently, one could argue that there is a bottleneck in the existing supply of EoL LIBs until the waste flow increases. Under these circumstances, recyclers would not be able to procure an increased amount of EoL LIBs, and therefore unable to obtain the potential revenue gains presented in scenario 1a and 1b. However, savings in mechanical processing operating costs could be obtained by processing cells instead of modules due to a decreased amount of processed material.

In contrast to scenario 1a and 1b, scenario 2a and 2b would not result in an increased amount of cells recycled. The number of cells recycled remains the same. Rather, removal of the module components prior to recycling would result in a reduced amount of materials processed in the mechanical process. As the same amount of cells are processed, and the module components are recovered during the robotic disassembly, processing of cells instead of modules would not result in any loss of recycling revenue. Instead, operating costs could be reduced due to the decreased volume of materials recycled. Based on these factors, potential cost savings for the small and large capacity mechanical processing steps of the LithoRec process are presented in scenarios 2a and 2b below.

Scenario 2a

An assumption is made that the supply of battery modules is limited to an amount equal to the small capacity class of the mechanical process. In other words, recyclers are unable to procure a higher amount of battery modules than 1,200 tons due to limited supply. By processing cells instead of modules for the Hyundai, the facility would process 949 tons of cells rather than 1,200 tons of modules, resulting in a 251 tons decrease in processed material.

LithoRec considers operating expenses to be proportional to throughput. Therefore, a decrease in throughput results in a reduction of operating costs. By assuming that the overall operating costs are directly proportional to throughput, a correlation function that depicts the operating costs per tonne of processed material can be used by treating the given operational costs for the two capacities, listed in Table 3.1, as two data points (view Appendix D.1). Consequently, the operating costs could be scaled down by using the annual throughput of 949 tons of material for the Hyundai as an input to interpolate the correlation function. Based on the scenario analysis, the revised operating cost is $370,872 compared to an operating cost of $385,664 at 1,200 tonne capacity, referring to Table 3.1. This translates to annual operation costs savings of $14,792 while yielding a NPV of $-323,698 for the robotic disassembly line. Results for the Volkswagen and the Mitsubishi are presented in Table 4.23. The graphical representation in Figure 4.10 highlights a comparison between processing modules and cells in scenario 2a.
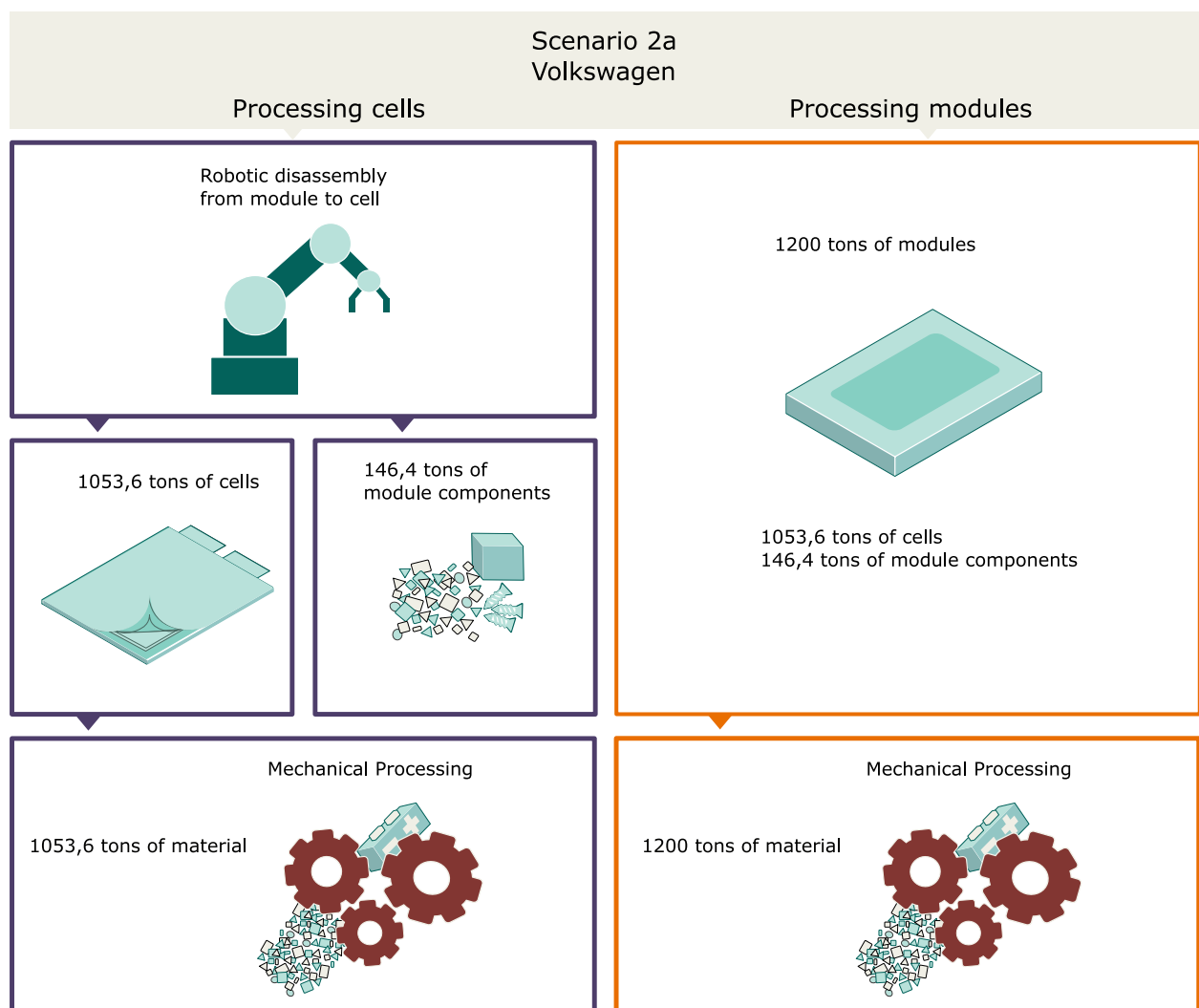
Figure 4.10: Illustration of scenario 2a.

Table 4.23: Parameters, scenario 2a

	Volkswagen	Hyundai	Mitsubishi
Decrease in processed material	147 [ton]	251 [ton]	148 [ton]
Annual cost savings	$8,631	$14,792	$8,707
NPV	$-350,101	$-323,698	$-348,292

Scenario 2b

Similar to scenario 2a, a bottleneck could be modelled for the large capacity class. In other words, an existing bottleneck in the supply of EoL EV LIBs leads to the conclusion that the amount of cells recycled can not be increased, in contrast to scenario 1a and 1b. This scenario is comparable with scenario 1b in that both cells and modules are processed due to the restrained capacity of the robotic disassembly line. The potential decrease in processed material and potential operating cost savings is controlled by the processing capacity of the robotic disassembly line.

The robotic disassembly line disassembles an annual amount of 2,314 tons of Hyundai battery modules, which translate into 1,829 tons of battery cells. Accordingly, the decrease of processed material equals 2,314 - 1,829 = 485 tons. Consequently, the facility processes 6,000 - 485 = 5,515 tons of material instead of 6,000 tons. The correlation function used in scenario 2a are again utilized to obtain the operating costs at the different volumes and potential operating cost savings, outlined in Appendix D.1. For the Hyundai, a revised operating cost of $639,546 are estimated compared to an operating cost of $668,069 at 6,000 tons capacity, referring to Table 3.1. On balance, this results in annual cost savings of $28,523, yielding a NPV of $-267,243 for the robotic disassembly line. Results for the Volkswagen and Mitsubishi are summarized in Table 4.24, and an illustration of the scenario is presented in Figure 4.11.
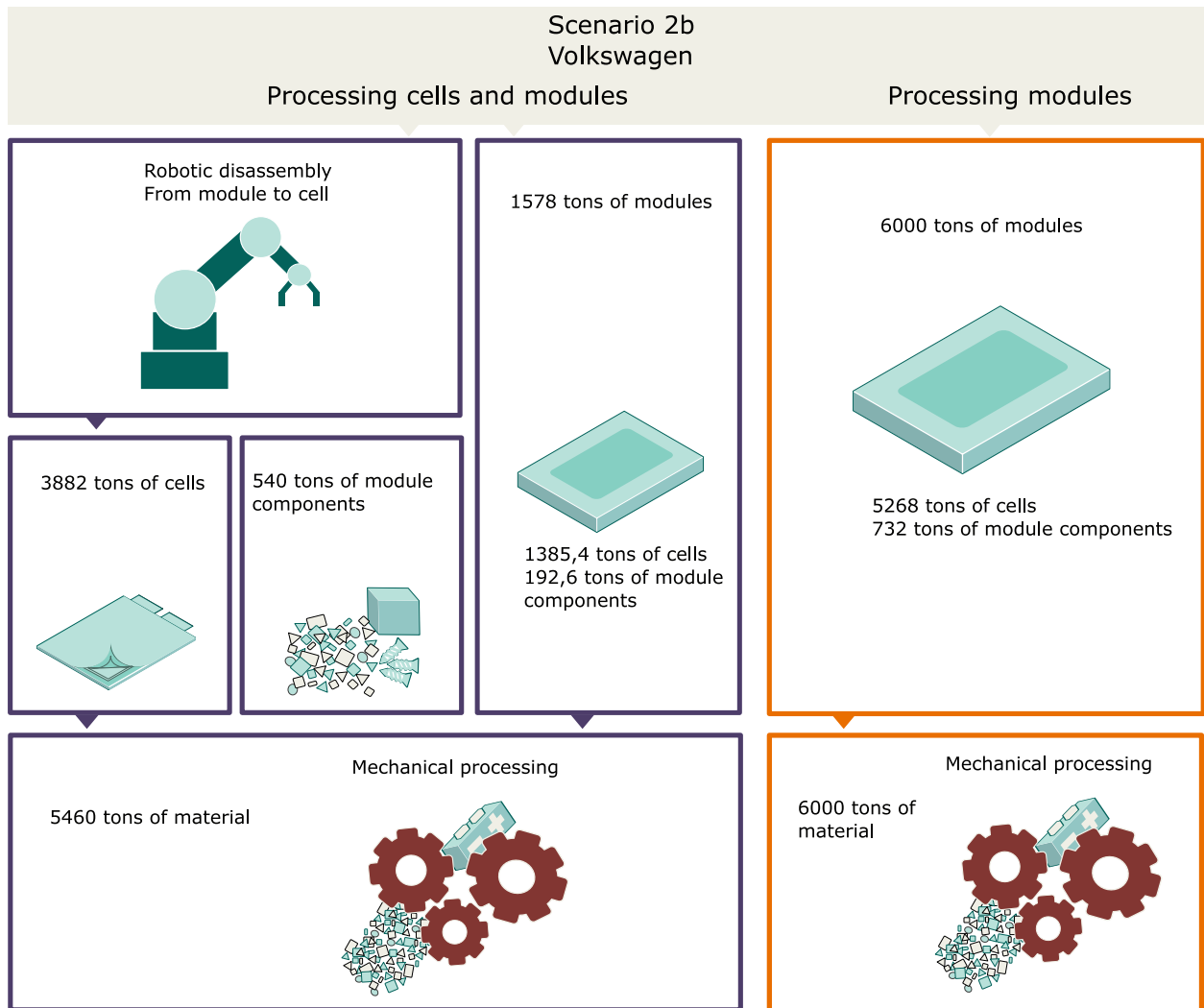
Figure 4.11: Illustration of scenario 2b.

Table 4.24: Parameters, scenario 2b

	Volkswagen	Hyundai	Mitsubishi
Decrease in processed material	540 [ton]	485 [ton]	387 [ton]
Annual cost savings	$31,804	$28,523	$22,761
NPV	$-254,825	$-267,243	$-290,510

4.2.3 Reduction of processing steps in recycling
Scenario 3

Processing of cells instead of modules could yield even further cost savings than the ones presented in Section 4.2.2. The flowchart of the LithoRec mechanical process depicted in Figure 2.4 indicates that steel is separated through a magnetic separation process after the modules are subjected to shredding and thermal drying. Given the absence of steel within the cells, as indicated in Table 3.3, disassembly of the modules could eliminate the need for this particular step in the recycling process. Consequently, this approach has the potential to yield cost savings in terms of both investment and operational cost if the magnetic separator were to be removed.

The required capacity of the magnetic separator needs to be determined in order to obtain the investment costs and operational costs of the equipment in question. Further, for the magnetic separator to be neglected, only pure cells can be subjected to the mechanical process due to the presence of steel in the module components. Thus, the large scale capacity plant is out of this scope, given that both cells and modules would be processed at this capacity. Consequently, a magnetic separator applicable for the small capacity process is reviewed.

Based on the dimensional specifications outlined in Table 4.2, the volume of the Volkswagen module amounts to $0.01m^3$. Considering the annual capacity of 1,200 tons, the yearly volumetric throughput of Volkswagen modules reaches $1,101m^3$. The operational schedule of the LithoRec recycling facility follows a 3-shift system, spanning 250 working days per year (Kwade & Diekmann, 2017). Hence, it is assumed that the equipment has an annual operating time of 6,000 hours.

To calculate the required hourly throughput of the separator, the annual volume of $1,101m^3$ is divided by the available operating time of 6000 hours per year. The electrolyte is the only material that is not contained during the mechanical process, and is therefore not included in the calculations. The resulting hourly flow rate for the Volkswagen module is $0.10m^3/h$.

Following consultations with an industrial retailer regarding magnetic separator drums, a cost estimation on a machine that satisfies the required hourly flow rate was obtained. The separator could be procured at a cost of \$35,000 with a capacity of processing $1.25m^3/h$. Based on projections from EverBatt on similar activities, the separator would require three hours of labor per day to be operated ("Argonne National Laboratory," n.d.). The annual cost savings from operational costs, including labor cost, a 2% maintenance fee of the in-

vestment cost and electricity charges, are expected to amount to $23,800. Additionally, the initial investment cost of the plant would decrease by $35,000, yielding a NPV of $-252,734 for the Volkswagen module. The same calculations have been applied to the modules of Hyundai and Mitsubishi, and the results are presented in Table 4.25.

Table 4.25: Parameters, scenario 3

	Volkswagen	Hyundai	Mitsubishi
Module volume	$0.01m^3$	$0.03m^3$	$0.02m^3$
Annual throughput	$618.67m^3$	$776.24m^3$	$707.96m^3$
Hourly flow rate	$0.10m^3/h$	$0.13m^3/h$	$0.12m^3/h$
Annual cost savings	$23,800	$23,800	$23,800
NPV	$-252,734	$-251,661	$-251,237

Integration of scenario 3 with previous scenarios

As previously stated, the mechanical separation process of steel is only necessary in scenarios where recycling plants processes modules or a combination of cells and modules. Therefore, scenarios with no modules present in the recycling process, has an opportunity to exclude the installation of a magnetic separator. With the current capacity of the robot disassembly line modelled in this article, only the small capacity plant could benefit from excluding an installation of a magnetic separator.

With this in mind, it is possible to revise scenario 1a by eliminating the magnetic separator. In the case of the Volkswagen module, the annual cash flow increases with $23,800 due to the decreased operational costs. Additionally, investment cost are decreased by $35,000 which in turn increases the NPV of scenario 1a to $3,017,119. Results are summarized in Table 4.26 and includes the Hyundai and Mitsubishi modules.

Table 4.26: Revised parameters, scenario 1a

Scenario 1 a	Volkswagen	Hyundai	Mitsubishi
Old annual revenue gain	$808,447	$1,165,489	$1,512,985
Old NPV	$2,938,268	$4,407,288	$5,836,408
Revised annual revenue gain	$832,247	$1,189,289	$1,536,785
Revised NPV	$3,017,119	$4,540,139	$5,969,259

Similar to scenario 1a, scenario 2a processes only pure cells. Conclusively, installation of the magnetic separator could be neglected, obtaining the same cost savings as presented in Table 4.26. Further results for the integration of scenario 3 with scenario 2a is summarized in Table 4.27 including the battery modules for Hyundai and Mitsubishi.

Table 4.27: Revised parameters, scenario 2a

Scenario 2 a	Volkswagen	Hyundai	Mitsubishi
Old annual cost savings	$8,631	$14,792	$8,707
Old NPV	$-350,101	$-323,698	$-348,292
Revised annual cost savings	$32,431	$38,772	$32,507
Revised NPV	$-217,248	$-190,105	$-215,439

Chapter 5

Discussions

This chapter reviews the significance of the findings and to what degree the findings can be useful. More specifically, the chapter reviews the findings pertaining to the cost of robotic disassembly, the potential annual throughput of EV modules, and the various scenarios that have been presented. Also, relevant scenarios that go beyond those already quantitatively presented will be discussed.

5.1   Cost of robotic disassembly

The proposed robotic module disassembly line is modelled in a highly structured robotic environment. That is, the throughput of battery modules are homogeneous. Consequently, the disassembly process would be a repetitive process based on pre-programmed robots, similar to the iPhone 6 disassembly line presented in Section 2.4.1 Given these conditions, a one off engineering cost to program the disassembly line would accrue the cost of robotic disassembly. While this might be true, pre-programmed robots does not solve the inherent challenges of automated robotic disassembly. Future robotic disassembly lines must handle mixed waste streams given the design variations in EV batteries. As emphasized in Section 2.4.1 and 2.4.2, this could be solved by either applying AI that can handle mixed waste streams, or increasing the degree of design for disassembly or standardizing battery design.

If the challenges were to be solved by AI, one could argue that investment costs or engineering development costs in AI software would accrue. On the other hand, standardization of battery design could yield a more structured robotic environment. Such an environment would arguably be similar to the environment modelled in this thesis. In like manner, if the battery labelling and design for disassembly were to be improved, the original car manufactures could pre-program the required disassembly sequence for different battery

modules. Consequently, scanning of the battery labels would allow for the proper disassembly sequence to be performed without the requirement for pre-programming or AI. Given that the original car manufacturer is familiar with the EV battery's structure, this would require less effort than having a third party carry out the disassembly sequence planning. In this hypothetical situation, the suggested robotic module disassembly line's projected cost is rather accurate.

Comparable results regarding cost of disassembly could be found in the literature. To begin with, Table 4.19 presents the disassembly cost per module and per kWh. First thing to remember, is that the cell to module weight ratio and the number of cells in the different modules varies. The Volkswagen module contains 12 cells with a weight ratio of 0.878, while the Hyundai module contains 40 cells with a weight ratio of 0.790 and the Mitsubishi module contains 16 cells with a weight ratio of 0.877. In light of these considerations, when comparing results to similar findings in the literature, the most comparable unit of measure is the cost per kWh instead of cost per module.

The study by Lander et al. (2023) was previously introduced in Section 1.2. The study examines the cost associated with disassembling various EV battery packs, from pack to cell level, for both manual and automated disassembly processes. One of the batteries that were analyzed is the Peugeot 208 e GT battery pack. The Peugeot 208 e GT battery module resembles the Volkswagen battery module used in this study, both in terms of number of cells, structure and module components. The results of the study shows that the cost of disassembling the Peugeot 208 e GT battery pack to cell level in a fully automated process accrues to \$0.11/kWh. Further interpretation of the study's results shows that 10.4% of these cost are related to disassembly from pack to module level, while the remaining 89.6% are related to disassembly from module to cell level. Consequently, according to Lander et al. (2023), disassembly cost for the Peugeot 208 e GT from module to cell level in a fully automated process accrues to \$0.11 x 0.896 = \$0.099/kWh. This is in close proximity to the computed cost per kWh for the Volkswagen outlined in this thesis, which is equivalent to \$0.137/kWh. However, this study has examined the expenses associated with the robotic module disassembly line, while the investigation conducted by Lander et al. (2023) is founded on the assumption that a fully automated disassembly line reduces the costs of manual disassembly by 97% without any modelling of a robotic disassembly line. Put differently, the disassembly costs modelled in this study is more comprehensive.

5.2   Annual throughput

According to Table 4.17, the estimated annual throughput of battery modules in the robotic disassembly line varies depending on module type. It should be noted, as previously stated, that the cell to module weight ratio and the number of cells present in the various modules are not constant. Therefore, throughput of modules does not reflect the amount of valuable cells disassembled in the disassembly line. Hence, the most compelling evidence to consider while discussing throughput of the robotic module disassembly line is the throughput of cells in tonne, as presented in Table 4.17.

Disassembly of the Hyundai module yields the lowest throughput in tonnes of cells. This is evident from the relatively low cell to module weight ratio. The Hyundai module is a rather complex structure. Obtaining the 40 cells requires removal of a significant amount of module components, referring to Table 4.7. The Volkswagen, on the other hand, has a larger cell to module weight ratio, implying that fewer module components are removed. At the same time, one could argue that the Hyundai module is the most viable to disassemble given the large amount of module components removed.

The variations in throughput builds to show the magnitude of design variations in EV batteries. It is arguable that the Volkswagen and the Mitsubishi, possessing a higher cell to module weight ratio, are better designed for disassembly compared to the Hyundai. Altogether, increased standardization in design or prioritizing design for disassembly could potentially mitigate the fluctuations in throughput.

As mentioned in Section 2.4, it is not anticipated that standardization in design will occur in the near future (Harper et al., 2019). Hence, scaling up the robotic module disassembly line represents a viable solution to the fluctuations in throughput. The disassembly line modelled in this thesis is based on minimum requirements and rather conservative estimates. It is highly probable that an increase in the capacity of the disassembly line can be achieved. One could argue that the relationship between the cost of the robotic disassembly line and its capacity may not be linear due to the potential for obtaining discounts on bulk purchases. Therefore, increasing the capacity of the disassembly line has the potential to decrease the cost of disassembly per kWh disassembled.

5.3 Economic viability

5.3.1 Improved capacity utilization

Scenario 1a

The data presented in Table 4.21 indicates a notable improvement in revenue generated through the processing of cells, as opposed to modules, across all three battery modules. Mitsubishi with valuable LCO chemistry exhibits a higher revenue of \$12.2 million in comparison to Hyundai's \$5.4 million. However, it is the extent of increase in revenue gain observed from cell processing that merits attention. Volkswagen's revenue increased by 14%, Mitsubishi's by 14%, and Hyundai's by a substantial 27%.

Hyundai's revenue gain is considerably greater than that of the Volkswagen and Mitsubishi, primarily due to its lower cell to module weight ratio in comparison to the latter two modules. In other words, processing Hyundai modules as input to the mechanical process would result in a relatively low number of cells being processed initially. However, when pure cells are fed to the mechanical process, the Hyundai yields a significantly higher quantity of additional valuable cell material.

Furthermore, it is worth noting that an increase in the quantity of processed cells corresponds proportionally with a rise of module components disassembled. Specifically, in the Hyundai's disassembly line, processing 1,200 tons of pure cells would result in a substantially greater quantity of module components compared to the quantities generated by the other two battery modules, potentially leading to increased revenue. All things considered, the NPV presents a positive outcome across the battery modules. Given the conditions set forth in scenario 1a, investing in a disassembly line for robotic modules is deemed economically viable.

To finish, the robotic disassembly line modelled in this study has a larger capacity than the small capacity mechanical process. The robotic disassembly line disassembles a significant surplus of battery modules. Specifically, regarding the Volkswagen module, the disassembly line has the capacity to process 3.24 times more tons of material than the mechanical process. In this scenario, the robotic disassembly line could be down-scaled, or the remaining disassembled cells could be sold to a third-party. The same applies for the Hyundai and the Mitsubishi.

Scenario 1b

Regarding scenario 1b, the mechanical process has a capacity limit of 6,000 tons of material, which the disassembly line is unable to match for all three battery modules. In this case, the input of pure cells is equivalent to the annual throughput of the disassembly line, while modules are added to reach the mechanical process capacity limit.

In this scenario, the revenue gains for Volkswagen, Mitsubishi, and Hyundai are 9%, 6%, and 8%, respectively. An area of interest is the discrepancy in revenue gains observed across module types as their capacity changed from 1,200 to 6,000. All battery modules experienced a percentage decrease in revenue gain compared to scenario 1a, with the most substantial decline observed in the case of Hyundai. That is, however, logical explained by the fact that modules are being used as well in the mechanical process in order to fully meet the capacity range of the mechanical process. Thus, this scenario is not able to fully utilize the potential of processing pure cells in the mechanical process. As an illustration, the disassembly line is capable of disassembling 1,829 tons of Hyundai cells in contrast to 3,882 tons of Volkswagen cells, representing 30.4% and 64.7% of the process capacity, respectively. As a result, the percentage revenue gain of Hyundai exhibits a substantial decline from scenario 1a to scenario 1b.

While Mitsubishi's disassembly line has a higher capacity limit of 2,750 tons of cells, which accounts for 45% of the process capacity, it yields a lower percentage revenue gain compared to Hyundai. This can be attributed, once again, to the low cell to module weight ratio of Hyundai, which results in a less efficient processing of modules. Therefore, even a small quantity of pure cells processed has a significant impact on revenue gain due to the low cell to module ratio.

In conclusion, the NPV of the robotic investment indicates a positive outcome for all battery modules. Therefore, considering the specified conditions in scenario 1a, investing in a robotic module disassembly line is in fact economically viable. Furthermore, if the robotic module disassembly line were to be expanded to accommodate the mechanical process's capacity, specifically for the processing of 6,000 tonnes of pure cells, the consequent growth in revenue gains would be substantial. This expansion would also result in a further increase in the NPV of the investment.

5.3.2 Cost reduction potential under current supply volumes

As previously indicated in Section 4.2.2, the recycling industry is preparing for the anticipated increase of EoL EV LIBs in the future. As highlighted in Section 1.1, the estimated number of such batteries is anticipated to escalate from 97,520 in 2023 to 1,103,764 by 2035 in the European Union, signifying a substantial growth trajectory. Consequently, recyclers must take proactive measures to cope with the projected volume. However, as scenarios 2a and 2b reveal, the quantity of recyclable spent LIBs is currently limited. As a result, there are currently few incentives for recyclers to expand operations to meet the projections. Hence, the objective of these two scenarios is not to explore potential revenue gains, but rather to determine whether the potential cost savings achieved by reducing the amount of materials processed in the mechanical process could be significant enough to justify investing in a robotic disassembly line scaled for future volumes. Thus, the question is whether such an investment is economically feasible at present times.

As indicated in Tables 4.23 and 4.24, when the bottleneck equals the processing capacity, reducing the amount of materials processed results in lower operational costs for the mechanical process. Nevertheless, the investment cost of the disassembly line is prohibitively high, and the NPV alone is not favorable. However, subsequent recycling stages, such as hydrometallurgical processes, may present opportunities for further cost savings. For example, certain steps, like leaching, could benefit from processing less material.

In conclusion, the scenario under examination does not yield a positive NPV within the designated six-year investment time frame alone. Nonetheless, it does shed light on the potential cost savings that may be realized in the presence of an inadequate supply of EoL EV LIBs. Therefore, it should be taken into consideration solely by stakeholders who are seeking to proactively prepare for the impending supply stream.

5.3.3 Reduction of processing steps in recycling

The third scenario explores the potential of reducing process steps in recycling. The findings suggest that cost savings could be obtained by removing the magnetic separator from the mechanical process.

In conclusion, the removal of a magnetic separator results in an annual cost savings of $23,800 for all three battery modules, as well as a reduction in investment costs by $35,000. This is illustrated in Table 4.26 and Table 4.27. The annual cost savings and investment cost

reduction are applicable in other scenarios as well, provided that the capacity of mechanical processing does not exceed the disassembly line. Therefore, in order to fully evaluate the economic feasibility, scenario 3 should not be considered in isolation, but rather as an extension for additional cost savings in the other scenarios. It is worthy of consideration that if the disassembly line were proportionately expanded to align with the mechanical process, the magnetic separation stage would become entirely superfluous and dispensable for all subsequent recycling operations.

5.3.4 Other scenarios

Additional scenarios that go beyond those already presented and discussed may also be relevant. However, due to constraints on data accessibility and collection, some scenarios have not been quantitatively presented, but they warrant mentioning. As stated in Section 1.2.1, this study focuses on analyzing the recycling option of EoL EV LIBs, opposed to other options as reuse and repurpose. However, disassembling modules to cell level could have advantages for the latter two options. Harper et al. (2019) argues that if an LIB module cannot easily be reused, it must be recycled. This is often due to inhomogeneous cell aging, resulting in a situation where only a few out-of-condition cells are enough to render an entire module unsuitable for reuse (Zhao et al., 2021). Rather, if the modules are disassembled to cell level, there exists a possibility of reusing cells that still are in good condition. To phrase it differently, cells that exhibit a diminished SoH could be recycled, whereas cells that possess a good SoH could be repurposed or reused. The adoption of this approach would not only offer environmental benefits but also contribute to an extended circular value chain, thus presenting the possibility of generating economic gains. This would, however, require accurate assessment of the SoH of the cells, which in turn implies the investment of both temporal and financial resources.

Another key point is the potential for increased recycling efficiency and purity of output materials in the mechanical processing steps. Sommerville et al. (2020) states that: "Effective separation of battery components, which produces enhanced purity of waste streams is essential to providing a cost-effective recycling process [...]. Improvements in the separation process are possible if the materials are separated prior to comminution, to prevent contamination of the different materials streams.". By processing cells instead of modules, the amount of extraneous material subjected to the mechanical processing steps is reduced. This can potentially enhance the purity of the output materials because there is less contamination from non-targeted materials. Consequently, recycling revenue could be increased.

Chapter 6

Conclusions

This study has shown that, automated disassembly of EV LIBs from module to cell level prior to recycling could be economically viable given certain circumstances. The assessed EV modules include the Volkswagen E-Golf 2019, Hyundai Ioniq 2. Gen 2019 and the Mitsubishi Outlander 2017. Based on a detailed teardown analysis of the battery modules, a robotic module disassembly line was modelled, and associated robotic disassembly times and costs were estimated. Further, using the mechanical processing steps of LithoRec as a reference recycling process, potential recycling revenues per kilo recycled cell was estimated in the EverBatt model. From this, potential scenarios that could increase recycling revenue or reduce recycling costs by mechanically processing cells instead of modules were established. Hence, this thesis adds to earlier techno-economic studies that have assessed LIB disassembly techniques and recycling processes (Alfaro-Algaba & Ramirez, 2020; Lander et al., 2023; Thompson et al., 2021) by conducting a more comprehensive modelling of the costs and benefits of an automated disassembly process.

The annual costs of the robotic module disassembly line was estimated at approximately $89,000, disassembling an annual amount of 405,878 Volkswagen modules, 52,686 Hyundai modules and 123,100 Mitsubishi modules. This translates to a disassembly cost per module of $0.22, $1.69 and $0.721, respectively. The potential annual revenue per kilo cell recycled was estimated at $5.38, $4.39 and $10.15, respectively.

The economic viability of the robotic module disassembly line is dependent on several factors. In general, the main findings indicate that processing of cells instead of modules could increase recycling revenue by 6% to 27% depending on processing capacity and type of module. As a consequence, the NPV of the robotic disassembly line was estimated to fall within the range of $2,938,268 to $13,862,214. This was based on the condition that the

volume of cells recycled is increased while still operating within a given recycling capacity. Considering the anticipated increase in the number of EoL EV LIBs in the future, this scenario gains even more relevance. Conversely, processing cells instead of modules at current supply volumes does not result in a positive NPV. Finally, it should be noted that additional cost savings were identified by avoiding certain process steps when processing cells instead of modules, which was subject to the condition that the cells did not contain any steel.

In conclusion, it can be stated that automated disassembly of EV LIBs to cell level is economically viable, particularly when considering the projected increase of EoL EV LIBs. The main reason for this is the increased amount of valuable materials that can be recovered by subjecting the cells to the recycling process. In contrast, processing modules limits recycling capacity due to the additional recycling of less valuable module components.

6.1 Limitations

Several limitations have curtailed the potential outcomes of this study, warranting explication. The primary limitations are twofold. First, in regard to the disassembly line and the modelling of battery module disassembly, and secondly, the dearth of available data for utilization in economic estimations.

Although the sampling of the battery modules used in this study considers three distinct variations of cell chemistry sourced from both BEV and PHEV from different manufacturers, this study is limited in its scope by solely examining three specific battery module designs. The limitation stems from the fact that there exists a number of variations in battery module design, even for modules with identical cell chemistries. Increasing the sample size may lead to a more comprehensive understanding of the economic feasibility of a robotic disassembly line for the entire spectrum of battery module designs. While this is true, the selected batteries are common battery types and gives a fair indication of the techno-economic viability of automated disassembly.

Secondly, the present study is limited by the availability of data regarding processes employed in the industry. Notably, the LithoRec process is one of the few, if not the sole, extensively documented recycling processes that are publicly accessible. Despite the widespread use of LithoRec in literature, it should be noted that this process was first projected in 2012, and certain aspects of it may have become outdated in comparison to advancements made by recyclers in the industry. Likewise, the EverBatt model represents another comprehensive

recycling model that is available to the public. In the current study, the EverBatt model was employed to derive the revenue per kg of recycled cell for the different cell chemistries. However, the model is based on a generic cathode composition, when in reality the cathode composition for one type of chemistry may vary. Hence, the result is limited to a generic value for each cathode material. Furthermore, it should be noted that the value of these materials is subject to variation over time, thus the revenue estimate is limited to the time at which it was calculated.

6.2 Future research

Further research is recommended to additionally verify the question of whether it is economically advantageous to stop EV LIB disassembly at the module or cell level. Such investigations should involve the development of a physical robotic disassembly line capable of validating the estimated disassembly time and annual throughput potential, or even refining them to a higher degree of accuracy. Moreover, given that the robotic disassembly line presented in this study was modelled in a highly structured environment, one may contend that the current direction of AI systems development could facilitate the creation of surpassing setup. Additionally, as mentioned in 6.1 future research could assess more battery designs and consider state of the art recycling processes as basis for the evaluation.

Another area for future research involves examining additional scenarios, such as estimating revenue of reusing individual cells with a high SoH within a module that would otherwise be considered to have a poor SoH. Moreover, the possibility of improving recycling efficiency and material purity through enhancements in the separation of battery components should also be considered for future research.

Bibliography

Ahuja, J., Dawson, L., & Lee, R. (2020). A circular economy for electric vehicle batteries: Driving the change. *Journal of Property, Planning and Environmental Law*, *12*, 235–250. https://doi.org/10.1108/JPPEL-02-2020-0011

Albertsen, L., Richter, J. L., Peck, P., Dalhammar, C., & Plepys, A. (2021). Circular business models for electric vehicle lithium-ion batteries: An analysis of current practices of vehicle manufacturers and policies in the eu. *Resources, Conservation and Recycling*, *172*, 105658. https://doi.org/10.1016/j.resconrec.2021.105658

Alfaro-Algaba, M., & Ramirez, F. J. (2020). Techno-economic and environmental disassembly planning of lithium-ion electric vehicle battery packs for remanufacturing. *Resources, Conservation and Recycling*, *154*, 104461. https://doi.org/10.1016/j.resconrec.2019.104461

Ali, H., Khan, H. A., & Pecht, M. (2022). Preprocessing of spent lithium-ion batteries for recycling: Need, methods, and trends. *Renewable and Sustainable Energy Reviews*, *168*, 112809. https://doi.org/10.1016/j.rser.2022.112809

Argonne National Laboratory. (n.d.). https://www.anl.gov/amd/everbatt

Austeng, K., Torp, O., Midtbø, J. T., Helland, V., & Jordanger, I. (2005). *Usikkerhetsanalyse - metode* (Concept rapport Nr 12). NTNU. https://ntnuopen.ntnu.no/ntnu-xmlui/handle/11250/228073

Bajolle, H., Lagadic, M., & Louvet, N. (2022). The future of lithium-ion batteries: Exploring expert conceptions, market trends, and price scenarios. *Energy Research and Social Science*, *93*, 102850. https://doi.org/10.1016/j.erss.2022.102850

Batteries Europe. (2020). *Strategic research agenda for batteries*. https://ec.europa.eu/newsroom/ener/items/696024

Bjørnenak, T. (2019). *Strategiske lønnsomhetsanalyser* (1st ed., Vol. 1). Fagbokforlaget.

Bocken, N. M. P., de Pauw, I., Bakker, C., & van der Grinten, B. (2016). Product design and business model strategies for a circular economy. *Journal of Industrial and Production Engineering*, *33*, 308–320. https://doi.org/10.1080/21681015.2016.1172124

Brückner, L., Frank, J., & Elwert, T. (2020). Industrial recycling of lithium-ion batteries—a critical review of metallurgical process routes. *Metals*, *10*, 1–29. https://doi.org/10.3390/met10081107

Chen, M., Ma, X., Chen, B., Arsenault, R., Karlson, P., Simon, N., & Wang, Y. (2019). Recycling end-of-life electric vehicle lithium-ion batteries. *Joule*, *3*, 2622–2646. https://doi.org/10.1016/j.joule.2019.09.014

Choux, M., Bigorra, E. M., & Tyapin, I. (2021). Task planner for robotic disassembly of electric vehicle battery pack. *Metals*, *11*, 1–18. https://doi.org/10.3390/met11030387

Cicconi, P., Landi, D., Morbidoni, A., & Germani, M. (2012). Feasibility analysis of second life applications for li-ion cells used in electric powertrain using environmental indicators. *2012 IEEE International Energy Conference and Exhibition, ENERGYCON 2012*, 985–990. https://doi.org/10.1109/EnergyCon.2012.6348293

Crooks, E. (2020). *What the coronavirus means for the energy transition | wood mackenzie*. https://www.woodmac.com/news/feature/what-the-coronavirus-means-for-the-energy-transition/

Datar, S. M., & Rajan, M. V. (2018). *Horngren's cost accounting : A managerial emphasis* (16th ed.). Pearson Education Limited.

Demandt, B. (2018). European sales 2017 ev and phev segments. *CARSALESBASE*. https://carsalesbase.com/european-sales-2017-ev-phev-segments/

Drevland, F. (2005). *Rett og riktig - en gjennomgang av statens vegvesen analysemodell* (Concept rapport Nr. 1070-6). NTNU. https://www.ntnu.no/documents/1261860271/1262021752/054_rapport_05_rett_og_riktig_forelopig.pdf

Element Energy. (2019). *Batteries on wheels: The role of battery electric cars in the eu power system and beyond.* https://www.transportenvironment.org/discover/batteries-wheels-role-battery-electric-cars-eu-power-system-and-beyond/

European Comission. (2022). Green deal: Eu agrees new law on more sustainable and circular batteries to support eu's energy transition and competitive industry. https://ec.europa.eu/commission/presscorner/detail/en/ip_22_7588

European Commission. (n.d.). Co emission performance standards for cars and vans. https://climate.ec.europa.eu/eu-action/transport-emissions/road-transport-reducing-co2-emissions-vehicles/co2-emission-performance-standards-cars-and-vans_en

European Commission. (2000). Directive 2000/53/ec of the european parliament and of the council of 18 september 2000 on end-of life vehicles. *The European Parliament and the Council of the European Union.* Retrieved February 20, 2023, from https://eur-lex.europa.eu/eli/dir/2000/53/oj

European Commission. (2006). Directive 2006/66/EC on batteries and accumulators and waste batteries and accumulators and repealing Directive 91/157/EEC. *The European Parliament and the Council of the European Union.* Retrieved February 20, 2023, from https://eur-lex.europa.eu/eli/dir/2006/66/oj

European Commission. (2020). Proposal for a regulation concerning batteries and waste batteries, repealing directive 2006/66/ec and amending regulation (eu) no 2019/1020. *The European Parliament and the Council of the European Union.* Retrieved February 20, 2023, from https://eur-lex.europa.eu/legal-content/EN/ALL/?uri=COM:2020:798:FIN

European Parliament. (2023). Batteries: Deal on new eu rules for design, production and waste treatment. Retrieved February 20, 2023, from https://www.europarl.europa.eu/news/en/press-room/20221205IPR60614/batteries-deal-on-new-eu-rules-for-design-production-and-waste-treatment

Giacomella, L. (2021). Techno-economic assessment (tea) and life cyclecosting analysis (lcca): Discussing methodological steps and integrability. *Insights into Regional Development, 3*, 176–197. https://jssidoi.org/ird/article/66

Glöser-Chahoud, S., Huster, S., Rosenberg, S., Baazouzi, S., Kiemel, S., Singh, S., Schneider, C., Weeber, M., Miehe, R., & Schultmann, F. (2021). Industrial disassembling as a key enabler of circular economy solutions for obsolete electric vehicle battery systems. *Resources, Conservation and Recycling, 174.* https://doi.org/10.1016/j.resconrec.2021.105735

Hall, D., Wappelhorst, S., Mock, P., & Lutsey, N. (2020). *European electric vehicle factbook 2019/2020.* THE INTERNATIONAL COUNCIL ON Clean Transportation. https://ec.europa.eu/eurostat/web/regions-and-cities/overview

Hannan, M. A., Hoque, M. M., Hussain, A., Yusof, Y., & Ker, P. J. (2018). State-of-the-art and energy management system of lithium-ion batteries in electric vehicle applications: Issues and recommendations. *IEEE Access, 6*, 19362–19378. https://doi.org/10.1109/ACCESS.2018.2817655

Harper, G., Sommerville, R., Kendrick, E., Driscoll, L., Slater, P., Stolkin, R., Walton, A., Christensen, P., Heidrich, O., Lambert, S., Abbott, A., Ryder, K., Gaines, L., & Anderson, P. (2019). Recycling lithium-ion batteries from electric vehicles. *Nature, 575*, 75–86. https://doi.org/10.1038/s41586-019-1682-5

He, F., Yang, Y., Tamberrino, D., & Yang, V. (2017). *China's battery challenge: A new solution to a growth problem.* Goldman Sachs Global Investment Research.

International Energy Agency. (2021). *Global ev outlook 2021: Accelerating ambitions despite the pandemic.* https://www.iea.org/reports/global-ev-outlook-2021

Kachate, N., Sharma, D., & Baidya, K. (2022). Material recovery in li-ion battery recycling: Case study. *Materials Today: Proceedings, 72*, 1498–1502. https://doi.org/10.1016/j.matpr.2022.09.377

Kamran, M., Raugei, M., & Hutchinson, A. (2021). A dynamic material flow analysis of lithium-ion battery metals for electric vehicles and grid storage in the uk: Assessing the impact of shared mobility and end-of-life strategies. *Resources, Conservation and Recycling*, *167*, 105412. https://doi.org/10.1016/j.resconrec.2021.105412

Kay, I., Farhad, S., Mahajan, A., Esmaeeli, R., & Hashemi, S. R. (2022). Robotic disassembly of electric vehicles' battery modules for recycling. *Energies*, *15*, 4856. https://doi.org/10.3390/en15134856

Kuppens, T., Dael, M. V., Vanreppelen, K., Thewys, T., Yperman, J., Carleer, R., Schreurs, S., & Passel, S. V. (2015). Techno-economic assessment of fast pyrolysis for the valorization of short rotation coppice cultivated for phytoextraction. *Journal of Cleaner Production*, *88*, 336–344. https://doi.org/10.1016/J.JCLEPRO.2014.07.023

Kwade, A., & Diekmann, J. (2017). *Recycling of lithium-ion batteries: The lithorec way* (1st ed., Vol. 1). Springer Cham. http://www.springer.com/series/10615

Lander, L., Cleaver, T., Rajaeifar, M. A., Nguyen-Tien, V., Elliott, R. J., Heidrich, O., Kendrick, E., Edge, J. S., & Offer, G. (2021). Financial viability of electric vehicle lithium-ion battery recycling. *iScience*, *24*, 102787. https://doi.org/10.1016/j.isci.2021.102787

Lander, L., Tagnon, C., Nguyen-Tien, V., Kendrick, E., Elliott, R. J., Abbott, A. P., Edge, J. S., & Offer, G. J. (2023). Breaking it down: A techno-economic assessment of the impact of battery pack design on disassembly costs. *Applied Energy*, *331*, 120437. https://doi.org/10.1016/j.apenergy.2022.120437

Li, J., Barwood, M., & Rahimifard, S. (2018). Robotic disassembly for increased recovery of strategically important materials from electrical vehicles. *Robotics and Computer-Integrated Manufacturing*, *50*, 203–212. https://doi.org/10.1016/j.rcim.2017.09.013

Lichtenberg Partners. (n.d.). Successive principle in essence. http://www.lichtenberg.org/successive-principle

Marshall, J., Gastol, D., Sommerville, R., Middleton, B., Goodship, V., & Kendrick, E. (2020). Disassembly of li ion cells—characterization and safety considerations of a recycling scheme. *Metals*, *10*, 1–22. https://doi.org/10.3390/met10060773

Martinez-Laserna, E., Gandiaga, I., Sarasketa-Zabala, E., Badeda, J., Stroe, D.-I., Swierczynski, M., & Goikoetxea, A. (2018). Battery second life: Hype, hope or reality? a critical review of the state of the art. *Renewable and Sustainable Energy Reviews*, *93*, 701–718. https://doi.org/10.1016/j.rser.2018.04.035

Marturi, N., Adjigble, M., Ortenzi, V., Rajasekaran, V., Corke, P., & Stolkin, R. (2018). Model-free and learning-free grasping by local contact moment matching. *2018 IEEE/RSJ International Conference on Intelligent Robots and Systems (IROS), Madrid, Spain*, 2933–2940. https://doi.org/10.1109/IROS.2018.8594226

Meng, K., Xu, G., Peng, X., Youcef-Toumi, K., & Li, J. (2022). Intelligent disassembly of electric-vehicle batteries: A forward-looking overview. *Resources, Conservation and Recycling*, *182*, 106207. https://doi.org/10.1016/j.resconrec.2022.106207

Nguyen, T. C. (2019). *Automated li-ion battery dismantling line (from module to cells)* (Master's thesis). University of Agder, Grimstad.

Olivetti, E. A., Ceder, G., Gaustad, G. G., & Fu, X. (2017). Lithium-ion battery supply chain considerations: Analysis of potential bottlenecks in critical metals. *Joule*, *1*, 229–243. https://doi.org/10.1016/j.joule.2017.08.019

Or, T., Gourley, S. W., Kaliyappan, K., Yu, A., & Chen, Z. (2020). Recycling of mixed cathode lithium-ion batteries for electric vehicles: Current status and future outlook. *Carbon Energy*, *2*, 6–43. https://doi.org/10.1002/cey2.29

Poschmann, H., Brüggemann, H., & Goldmann, D. (2021). Fostering end-of-life utilization by information-driven robotic disassembly. *Procedia CIRP*, *98*, 282–287. https://doi.org/10.1016/j.procir.2021.01.104

Rhinoceros. (n.d.). Context - rhinoceros project. Retrieved May 14, 2023, from https://www.rhinoceros-project.eu/context/

Rouhi, H., Karola, E., Serna-Guerrero, R., & Santasalo-Aarnio, A. (2021). Voltage behavior in lithium-ion batteries after electrochemical discharge and its implications on the safety of recycling processes. *Journal of Energy Storage*, *35*, 102323. https://doi.org/10.1016/j.est.2021.102323

Schäfer, J., Singer, R., Hofmann, J., & Fleischer, J. (2020). Challenges and solutions of automated disassembly and condition-based remanufacturing of lithium-ion battery

modules for a circular economy. *Procedia Manufacturing*, *43*, 614–619. https://doi.org/10.1016/j.promfg.2020.02.145

Schumacher, P., & Jouaneh, M. (2013). A system for automated disassembly of snap-fit covers. *International Journal of Advanced Manufacturing Technology*, *69*, 2055–2069. https://doi.org/10.1007/s00170-013-5174-8

Schwarz, T. E., Rübenbauer, W., Rutrecht, B., & Pomberger, R. (2018). Forecasting real disassembly time of industrial batteries based on virtual mtm-uas data. *Procedia CIRP*, *69*, 927–931. https://doi.org/10.1016/j.procir.2017.11.094

Sommerville, R., Shaw-Stewart, J., Goodship, V., Rowson, N., & Kendrick, E. (2020). A review of physical processes used in the safe recycling of lithium ion batteries. *Sustainable Materials and Technologies*, *25*, e00197. https://doi.org/10.1016/j.susmat.2020.e00197

Sommerville, R., Zhu, P., Rajaeifar, M. A., Heidrich, O., Goodship, V., & Kendrick, E. (2021). A qualitative assessment of lithium ion battery recycling processes. *Resources, Conservation and Recycling*, *165*, 105219. https://doi.org/10.1016/j.resconrec.2020.105219

Stahel, W. R. (2016). The circular economy. *Nature*, *531*, 435–438. https://doi.org/10.1038/531435a

Statista. (2023). Ev batteries: Expected end-of-life stock eu 2018-2030. *Statista*. Retrieved May 4, 2023, from https://www.statista.com/statistics/1012083/ev-batteries-expected-end-of-life-stock-eu/

Thompson, D., Hartley, J. M., Lambert, S. M., Shiref, M., Harper, G. D., Kendrick, E., Anderson, P., Ryder, K. S., Gaines, L., & Abbott, A. P. (2020). The importance of design in lithium ion battery recycling-a critical review. *Green Chemistry*, *22*, 7585–7603. https://doi.org/10.1039/d0gc02745f

Thompson, D., Hyde, C., Hartley, J. M., Abbott, A. P., Anderson, P. A., & Harper, G. D. (2021). To shred or not to shred: A comparative techno-economic assessment of lithium ion battery hydrometallurgical recycling retaining value and improving circularity in lib supply chains. *Resources, Conservation and Recycling*, *175*, 105741. https://doi.org/10.1016/j.resconrec.2021.105741

Umeda, Y., Miyaji, N., Shiraishi, Y., & Fukushige, S. (2015). Proposal of a design method for semi-destructive disassembly with split lines. *CIRP Annals - Manufacturing Technology*, *64*, 29–32. https://doi.org/10.1016/j.cirp.2015.04.045

UNFCCC. (n.d.). The paris agreement | unfccc. https://shorturl.at/dlyRV

United Nations. (n.d.). The paris agreement | united nations. https://www.un.org/en/climatechange/paris-agreement

US EPA. (2023). Sources of greenhouse gas emissions. *United States Environmental Protection Agency*. Retrieved May 11, 2023, from https://www.epa.gov/ghgemissions/sources-greenhouse-gas-emissions

Wegener, K., Andrew, S., Raatz, A., Dröder, K., & Herrmann, C. (2014). Disassembly of electric vehicle batteries using the example of the audi q5 hybrid system. *Procedia CIRP*, *23*, 155–160. https://doi.org/10.1016/j.procir.2014.10.098

Wegener, K., Chen, W. H., Dietrich, F., Dröder, K., & Kara, S. (2015). Robot assisted disassembly for the recycling of electric vehicle batteries. *Procedia CIRP*, *29*, 716–721. https://doi.org/10.1016/j.procir.2015.02.051

Wei, Q., Wu, Y., Li, S., Chen, R., Ding, J., & Zhang, C. (2023). Spent lithium ion battery (lib) recycle from electric vehicles: A mini-review. *Science of The Total Environment*, *866*, 161380. https://doi.org/10.1016/j.scitotenv.2022.161380

World Economic Forum. (2019). *A vision for a sustainable battery value chain in 2030: Unlocking the full potential to power sustainable development and climate change mitigation*. https://shorturl.at/otAN3

Wrålsen, B., Prieto-Sandoval, V., Mejia-Villa, A., O'Born, R., Hellström, M., & Faessler, B. (2021). Circular business models for lithium-ion batteries - stakeholders, barriers, and drivers. *Journal of Cleaner Production*, *317*, 128393. https://doi.org/10.1016/j.jclepro.2021.128393

Xiong, S., Ji, J., & Ma, X. (2020). Environmental and economic evaluation of remanufacturing lithium-ion batteries from electric vehicles. *Waste Management*, *102*, 579–586. https://doi.org/10.1016/j.wasman.2019.11.013

Yoon, J. S. (2022). *Hyundai motor group's share in the global electric vehicle market from 2014 to the first half 2019*. Statista. https://www.statista.com/statistics/1099941/hyundai-kia-electric-vehicle-global-market-share/

Zhao, Y., Pohl, O., Bhatt, A. I., Collis, G. E., Mahon, P. J., Rüther, T., & Hollenkamp, A. F. (2021). A review on battery market trends, second-life reuse, and recycling. *Sustainable Chemistry*, *2*, 167–205. https://doi.org/10.3390/suschem2010011

Zimmermann, A. W., Wunderlich, J., Müller, L., Buchner, G. A., Marxen, A., Michailos, S., Armstrong, K., Naims, H., McCord, S., Styring, P., Sick, V., & Schomäcker, R. (2020). Techno-economic assessment guidelines for co2 utilization. *Frontiers in Energy Research*, *8*. https://doi.org/10.3389/fenrg.2020.00005

Appendix A

Excel workbook on GitHub

The Excel workbook used in this thesis can be accessed and downloaded using the QR-code or the following URL: https://github.com/Master-thesis-UiA-2023/Automated-disassembly

Figure A.1: GitHub QR code

Robotic cycle times

B.1 Robotic cycle times, Volkswagen

Robot identifier	Operational probability density per robot				Probability density	Time [s]	Std. [t]
	P(50) [t]	Std. [t]	P(90) [t]		P(50) disassembly	68,61	6,68
IRB6660	47,36	6,22	55,33		P(50) sum operation	117,93	8,08
GoFa	19,33	2,54	22,59		P(90) disassembly	77,17	
Swifty	52,24	4,51	58,02		P(90) operation	128,29	

Step	Description	Tool	Worst case	Most likely	Best case	E	Std.	E-OP
	Remove top cover							
1,1	Move to object	Mill	2	1	0,5	1,20661157	0,59288538	
1,2	2x Cut (top cover 35cm)		14	8	5	9,23966942	3,55731225	
1,3	Move between cuts		1	0,8	0,5	0,75867769	0,19762846	
1,4	Move to start position *		1,5	1	0,5	1	0,39525692	
1,5	Move to object *	Phillips	2	1	0,5	1,20661157	0,59288538	
1,6	Unscrew 1 screw		2,5	2	1	1,79338843	0,59288538	
1,7	Release screw		2	1,5	0,8	1,41735537	0,4743083	
1,8	Move to start position *		1,5	1	0,5	1	0,39525692	
1,9	Move to object *	Suction	2	1	0,5	1,20661157	0,59288538	
1,11	Grip and lift plastic cover		3	2	1	2	0,79051383	
1,12	Remove and release (plastic cover) *		2	1,5	0,8	1,41735537	0,4743083	
1,13	Move to start position *		1,5	1	0,5	1	0,39525692	
	Sum of time		35	21,8	12,1	23,246281		16,4157025
	Remove compression plates							
2,1	Move to object *	Mill	2	1	0,5	1,20661157	0,59288538	
2,2	2x Cut compression plate		8	4	3	5,23966942	1,97628458	
2,3	Move between cuts		2	1	0,5	1,20661157	0,59288538	
2,4	Move to start position *		1,5	1	0,5	1	0,39525692	
2,5	Change tool *	Gripper	10	7,5	5	7,5	1,97628458	
2,6	Move to object *		2	1	0,5	1,20661157	0,59288538	
2,7	2x Grip and lift (Compression plate)		6	4	2	4	1,58102767	
2,8	Remove and release (compression plate)		2	1,5	0,8	1,41735537	0,4743083	
2,9	Move to object (between compression plate)		2	1	0,5	1,20661157	0,59288538	
2,11	Remove and release (compression plate) *		2	1,5	0,8	1,41735537	0,4743083	
2,12	Move to start position *		1,5	1	0,5	1	0,39525692	
	Sum time		39	24,5	14,6	26,4008264		13,0702479
	Cut bridge between cells							
3,1	Move to object *	Mill	2	1	0,5	1,20661157	0,59288538	
3,2	20x Cut (2x Bridge)		22	16,5	11	16,5	4,34782609	
3,3	Move between Cut (between bridge)		1	0,8	0,5	0,75867769	0,19762846	
3,4	4x Cut (connectors & orange plastic)		4	3	2	3	0,79051383	
3,5	4x Move between cuts (connectors)		4	3,2	2	3,03471074	0,79051383	
3,6	Move to start position *		1,5	1	0,5	1	0,39525692	
	Sum time		34,5	25,5	16,5	25,5		23,2933884
	Remove CMC unit							
	Change tool*	Suction	10	7,5	5	7,5	1,97628458	
4,1	Move to object *		2	1	0,5	1,20661157	0,59288538	
4,2	Grip and lift (plastic cover)		3	2	1	2	0,79051383	
4,3	Remove and release (plastic cover *		2	1,5	0,8	1,41735537	0,4743083	
4,4	Move to start position *		1,5	1	0,5	1	0,39525692	
	Sum time		18,5	13	7,8	13,1239669		2
	Remove side module junction							
5,1	Change tool *	Flat head	10	7,5	5	7,5	1,97628458	
5,2	Move to object *		2	1	0,5	1,20661157	0,59288538	
5,3	2x Remove side module junction (by force)		4	3	2	3	0,79051383	
5,4	Move to object		2	1	0,5	1,20661157	0,59288538	
5,5	Move to start position *		1,5	1	0,5	1	0,39525692	
5,6	Change tool *	Gripper	10	7,5	5	7,5	1,97628458	
5,7	Move to object *		2	1	0,5	1,20661157	0,59288538	
5,8	2x Grip and lift (side module junction)		3	2	1	2	0,79051383	
5,9	Remove and release (side module junction)		2	1,5	0,8	1,41735537	0,4743083	
5,11	Move to object (side module junction)		2	1	0,5	1,20661157	0,59288538	
5,12	Remove and release (side module junction) *		2	1,5	0,8	1,41735537	0,4743083	
5,13	Move to start position *		1,5	1	0,5	1	0,39525692	
	Sum time		42	29	17,6	29,661157		8,83057851
	Preparation time							
5,1	New module					5	0	
	Sum of time					5		5

Figure B.1: Robotic cycle times for Volkswagen

B.2 Robotic cycle times, Hyundai

Robot	Operational probability density per robot					Probability density	Time [s]	Std. [t]
Identifier	P(50) [t]		Std. [t]	P(90) [t]		P(50) disassembly	218,63	27,91
IRB6660	80,75		9,93	93,47		P(50) sum operation	247,62	28,51
GoFa	124,69		26,39	158,51		P(90) disassembly	254,41	
Swifty	28,15		3,87	33,12		P(90) operation	284,16	

Step	Description	Tool	Worst	Most likely	Best	E	Std.	E-OP
	Remove top metal cover							
1,1	Move to object	Mill	2	1	0,5	1,206612	0,592885	
1,2	2x Cut (top metal cover 50cm)		20	10	7	12,89256	5,13834	
1,3	Move between cuts		1	0,8	0,5	0,758678	0,197628	
1,4	Move to start position*		1,5	1	0,5	1	0,395257	
1,5	Move to object (top metal cover)*	Suction	2	1	0,5	1,206612	0,592885	
1,6	Grip and lift		3	2	1	2	0,790514	
1,7	Remove and release		2	1	0,5	1,206612	0,592885	
1,8	Move to start position*		1,5	1	0,5	1	0,395257	
	Sum		33	17,8	11	21,27107		18,0644628
	Remove top plastic cover							
2,1	Move to object*	Mill	2	1	0,5	1,206612	0,592885	
2,2	2x Cut (top plastic cover 20cm)		10	5	4	6,652893	2,371542	
2,3	Move between cuts		1	0,8	0,5	0,758678	0,197628	
2,4	Move to start position*		1,5	1	0,5	1	0,395257	
2,5	Move to object*	Suction	2	1	0,5	1,206612	0,592885	
2,6	2x Grip and lift		6	4	2	4	1,581028	
2,7	Remove and release		2	1	0,5	1,206612	0,592885	
2,8	Move to object		2	1	0,5	1,206612	0,592885	
2,9	Remove and release*		2	1	0,5	1,206612	0,592885	
2,11	Move to start position*		1,5	1	0,5	1	0,395257	
	Sum		30	16,8	10	19,44463		13,8247934
	Remove CMC unit							
3,1	Move to object (cell terminal first time)*	12" cup	2	1	0,5	1,206612	0,592885	
3,2	28x unscrew bolts (cell terminal)		70	56	28	50,21488	16,60079	
3,3	27x Release bolts		54	40,5	21,6	38,2686	12,80632	
3,4	27x Move to object (cell terminal)		54	27	13,5	32,57851	16,00791	
3,5	Release bolts*		2	1,5	0,8	1,417355	0,474308	
3,6	Move to start position*		1,5	1	0,5	1	0,395257	
3,7	Move to object*	Mill	2	1	0,5	1,206612	0,592885	
3,8	2x Cut (plastic casing 60cm)		20	10	7	12,89256	5,13834	
3,9	3x Cut (plastic casing 18cm)		15	7,5	6	9,979339	3,557312	
3,11	4x Move between cuts		4	3,2	2	3,034711	0,790514	
3,12	18x Cut CMC connectors		18	13,5	9	13,5	3,557312	
3,13	18x Move between cuts		18	14,4	9	13,6562	3,557312	
3,14	Move to start position*		1,5	1	0,5	1	0,395257	
3,15	Change tool*	Gripper	10	7,5	5	7,5	1,976285	
3,16	Move to object (CMC-plastic casing)*		2	1	0,5	1,206612	0,592885	
3,17	2x Grip and lift		6	4	2	4	1,581028	
3,18	Remove and release		2	1	0,5	1,206612	0,592885	
3,19	Move to object		2	1	0,5	1,206612	0,592885	
3,21	Remove and release*		2	1	0,5	1,206612	0,592885	
3,22	Move to start position*		1,5	1	0,5	1	0,395257	
	Sum		287,5	194,1	108,4	197,2818		180,538017
	Extract cells							
4,1	Move to object (cells)*	Gripper	2	1	0,5	1,206612	0,592885	
4,2	Grip and lift (individual cell)		3	2	1	2	0,790514	
4,3	Remove and release*		2	1	0,5	1,206612	0,592885	
4,4	Move to start position*		1,5	1	0,5	1	0,395257	
4,5	Positioner flip over		2	1	0,5	1,206612	0,592885	
4,6	Cell falls out		5	3	1	3	1,581028	
	Sum of time		15,5	9	4	9,619835		6,20661157
	Preparation time							
5,1	New module						5	0
	Sum of time						5	

Figure B.2: Robotic cycle times for Hyundai

Robot	Operational probability density per robot				Probability density	Time [s]	Std. [t]
Identifier	P(50) [t]	Std. [t]	P(90) [t]		P(50) disassembly	517,72	59,88
IRB6660	203,62	44,21	260,28		P(50) sum operation	634,70	63,58
GoFa	80,50	14,83	99,50		P(90) disassembly	594,46	
Swifty	350,58	43,21	405,96		P(90) operation	716,18	

Step	Description	Tool	Worst	Most likely	Best	E	Std.	E-OP
	Remove top metal cover							
1,1	Move to object	Mill	2	1	0,5	1,206612	0,592885	
1,2	4x Cut(metal holder)		4	3	2	3	0,790514	
1,3	3x move between clips		2	1	0,8	1,330579	0,474308	
1,4	Move to start position*		1,5	1	0,5	1	0,395257	
1,5	Move to object (metal cover)*	Suction	2	1	0,5	1,206612	0,592885	
1,6	2x Grip and lift metal cover		6	4	2	4	1,581028	
1,7	2x Remove and release metal cover		4	3	1,6	2,834711	0,948617	
1,8	Move to object (metal cover)		2	1	0,5	1,206612	0,592885	
1,9	Move to start position*		1,5	1	0,5	1	0,395257	
	Sum of time		25	16	8,9	16,78512		13,57851
	Seperate cell towers & cell frames							
2,1	Change tool *	Umbraco	10	7,5	5	7,5	1,976285	
2,2	Move to object (inside umbraco "cylinder")*		3	2	1,5	2,206612	0,592885	
2,3	18x unscrew screw		45	36	18	32,28099	10,67194	
2,4	17x move between screws		51	34	25,5	37,5124	10,07905	
2,6	Move to start position*		1,5	1	0,5	1	0,395257	
	Sum of time		110,5	80,5	50,5	80,5		69,79339
	Seperate cells							
3,1	Move to object (Side of module) *	Mill	2	1	0,5	1,206612	0,592885	
3,2	4x vertical cut (welded brackets + cell attachment)		60	32	24	40,26446	14,22925	
3,3	3x move between cuts		6	3	1,5	3,619835	1,778656	
3,4	Move to start position *		1,5	1	0,5	1	0,395257	
	Sum of time		69,5	37	26,5	46,09091		43,8843
	Extract cells							
4,1	Move to object (First time)	Mill	2	1	0,5	1,206612	0,592885	
4,2	9x Move to object*		18	9	4,5	10,8595	5,335968	
4,3	10x4 cut (metal cell cover)		160	80	60	104,7934	39,52569	
4,4	10x2 Movement between cut		40	20	10	24,13223	11,85771	
4,5	10x Move to start position *		15	10	5	10	3,952569	
4,6	10x Change tool *	Suction	100	75	50	75	19,76285	
4,7	10x Move to object *		15	10	5	10	3,952569	
4,8	10x2 Remove metal cell cover		60	40	20	40	15,81028	
4,9	10x Move to object (between cell cover)		20	10	5	12,06612	5,928854	
4,11	10x2 Move to object (cell extraction)		40	20	10	24,13223	11,85771	
4,12	10x2 extraction cells		60	40	20	40	15,81028	
4,13	10x Change tool (to gripper)		100	75	50	75	19,76285	
4,14	10x2 Move to object (cell casing)		40	20	10	24,13223	11,85771	
4,15	10x2 Remove cell casing		60	40	20	40	15,81028	
	Sum of time		730	450	270	491,3223		385,4628
	Preparation time							
5,1	New module					5	0	
	Sum of time					5		5

Figure B.3: Robotic cycle times for Mitsubishi

Appendix C

Electricity cost

VW E-Golf 2019			
Robot	Operating time (sec)	Annual OP. time [h]	Power consumption [kW]
IRB 6660	55,33	6237,76	6237,76
GoFa	22,59	2547,04	1273,52
Swifty	58,02	6541,67	3270,83
Sum			10782,12
Cost			**$2 185,41**

Hyundai Ionic 2. Gen			
Robot	Operating time (P90)	Annual OP. time [h]	Power consumption [kW]
IRB 6660	260,28	3809,22	3809,22
GoFa	99,50	1456,24	728,12
Swifty	405,96	5941,18	2970,59
Sum			7507,93
Cost			**$1 857,99**

Mitsubishi Outlander			
Robot	Operating time (P90)	Annual OP time [h]	Power consumption [kW]
IRB 6660	93,47	3196,49	3196,49
GoFa	158,51	5420,59	2710,29
Swifty	33,12	1132,47	566,24
Sum			6473,02
Cost			**$1 754,50**

Variable electricity cost	0,062
Fixed net cost	1107,2
Variable net cost	0,038
Cost per kWh	$0,1
Power consumption IRB 6660 [kWh]	1,0
Power consumption GoFa [kWh]	0,5
Power consumption Swifti [kWh]	0,5
VW throughput	405878
Hyundai throughput	52686
Mitsubishi troughput	123110

Figure C.1: Annual electricity cost for disassembling the different modules

Appendix D

Recycling calculations

D.1 Interpolation

Scenario 2a					
BM	Module weight [kg]	Cell weight [kg]	Ratio	Recycled cells weight [tons]	Interpolation	Cost saving
Volkswagen	10,90	9,56	0,878	1053,30	377033,2305	8630,769548
Hyundai	43,92	34,72	0,790	948,59	370872,49	14791,51001
Mitsubishi	25,48	22,34	0,877	1052,01	376957,3069	8706,693127

Scenario 2b							
BM	Module weight [kg]	Cell weight [kg]	Ratio	Recycled modules weight	Recycled cells weight [tons]	Interpolation op. Costs	Interpolation reviced op. Cost	Cost saving
Volkswagen	10,90	9,56	0,878	4422,000	3881,43	575228,36	543423,9705	31804,39
Hyundai	43,92	34,72	0,790	2314,000	1829,20	451205,49	422682,532	28522,96
Mitsubishi	25,48	22,34	0,877	3137,000	2750,14	499626,18	476865,4374	22760,75

Plant capacity		
	Large	Small
Operating costs	668069	385664
Capacity	6000	1200

Figure D.1: Interpolation estimation for operating costs

D.2 Revenue gain calculation, scenario 1b

Module	Modules disassembled	Weight module [g]	Weight cell [g]	Nr. of cells pr module	Total weight modules [ton]	Total weight cells [ton]	Weight ratio	Revised cell throughput *	Revenue cell [kg cell]
VW E-Golf	405878	10896	797	12	4422	3882	0,878	5267	$ 5,38
Hyundai	52686	43922	868	40	2314	1829	0,790	4743	$ 4,39
Mitsubishi	123110	25478	1396	16	3137	2750	0,877	5260	$ 10,15

* Throughput of cells when processing modules

Processing modules only			
	Revenue cell components	Revenue module components	Sum
VW E-Golf	$ 28 333 877	$ 226 626	$ 28 560 502
Hyundai	$ 20 821 566	$ 531 591	$ 21 353 157
Mitsubishi	$ 53 389 685	$ 128 239	$ 53 517 924

Potential revenue gain	
	Hydrometallurgy
VW E-Golf	$ 2 639 217
Hyundai	$ 1 777 568
Mitsubishi	$ 3 465 067

Processing modules and cells			
	Revenue cell components	Revenue module components	Sum
VW E-Golf	$ 30 886 035	$ 313 684	$ 31 199 719
Hyundai	$ 22 504 901	$ 625 824	$ 23 130 725
Mitsubishi	$ 56 829 730	$ 153 261	$ 56 982 991

Figure D.2: Calculation of revenue gain in scenario 1b

D.2.1 Quantity of module components, scenario 1b

Module component parameters for processing modules and cells					Module component parameters for processing of modules only			
Aluminium	**Plastic**	**Steel**	**Sum**		**Aluminium**	**Plastic**	**Steel**	**Sum**
VW E-Golf 164	280	888	1332	**VW E-Golf *** 164	280	888	1332
Ratio 0,123	0,210	0,667	1,000	**Ratio **** 0,123	0,210	0,667	1,000
Sum total 92,067	199,393	572,314	863,774	**Sum total** 90,308	154,185	488,987	733,480
Hyundai 2564	3915	2753	9232	**Hyundai** 2564	3915	2753	9232
Ratio 0,278	0,424	0,298	1,000	**Ratio** 0,278	0,424	0,298	1,000
Sum total 328,805	502,056	353,042	1183,902	**Sum total** 349,119	533,074	374,854	1257,047
Mitsubishi 0	1106	2036	3142	**Mitsubishi** 0	1106	2036	3142
Ratio 0,000	0,352	0,648	1,000	**Ratio** 0,000	0,352	0,648	1,000
Sum total 0,000	249,026	458,423	707,449	**Sum total** 0,000	260,460	479,472	739,932
Value $ 1,45	$ 0,10	$ 0,28		**Value** $ 1,45	$ 0,10	$ 0,28	
Recovery 0,8	0,8	0,8		**Recovery ***** 0,8	0,8	0,8	

	VW E-Golf	Hyundai	Mitsubishi	
Cells	3882	1829	2750	Weight of diassembled cells
Modules	2118	4171	3250	Weight of modules as input in scenario 1b
Sum	6000	6000	6000	Sum of modules and cells
Cells org.	5267	4743	5260	The original amount of cells recycled
Cells new	5741	5126	5599	The new amount of cells recycled
Addi. Cells.	475	383	339	Sum of additional cells recycled

*Amount per module
** Ratio per module
*** Recovery rate when recycling module components, as of LithoRec

Figure D.3: Calculation of quantity of module components in scenario 1b

D.3 Net present value analysis

Revenue parameters	
Module	VW E-Golf
Recycling process	Hydrometallurgy

Potential revenue gain	$ 2 639 217

Payback time of robotic disassembly line							
Year	0	1	2	3	4	5	6
Investement cost	$ 325 197						
Operating costs	0	$ 14 688	$ 14 688	$ 14 688	$ 14 688	$ 14 688	$ 14 688
Revenue gain	0	$ 2 639 217	$ 2 639 217	$ 2 639 217	$ 2 639 217	$ 2 639 217	$ 2 639 217
Cash flow	$ -325 197	$ 2 624 529	$ 2 624 529	$ 2 624 529	$ 2 624 529	$ 2 624 529	$ 2 624 529
Cumulative cash flow	$ -325 197	$ 2 299 332	$ 4 923 861	$ 7 548 391	$ 10 172 920	$ 12 797 449	$ 15 421 978
Net present value analysis							
Discount rate	12 %						
Net present value	$ 10 465 312						

Figure D.4: Net present value analysis for scenario 1b